

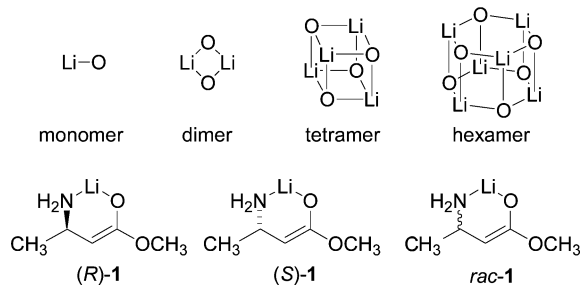
Characterization of β -Amino Ester Enolates as Hexamers via ${}^6\text{Li}$ NMR Spectroscopy

Anne J. McNeil,[†] Gilman E. S. Toombes,[‡] Sithamalli V. Chandramouli,[§] Benoit J. Vanasse,[§] Timothy A. Ayers,[§] Michael K. O'Brien,[§] Emil Lobkovsky,[†] Sol M. Gruner,[‡] John A. Marohn,[†] and David B. Collum*,[†]

Department of Chemistry and Chemical Biology, Baker Laboratory, Cornell University, Ithaca, New York 14853-1301, Physics Department, Clark Hall, Cornell University, Ithaca, New York 14853-2501, and Aventis, Process Development Chemistry, Bridgewater, New Jersey 08807

Received February 11, 2004; E-mail: dbc6@cornell.edu

As part of a program to prepare new antithrombotic agents, we discovered that unprotected β -amino esters can be exclusively C-alkylated. We sought to optimize this process by studying the structures and reactivities of β -amino ester enolates.¹ Determining the aggregation state of an enolate, however, is especially difficult due to the high symmetry of the possible aggregates—monomers, dimers, tetramers, and hexamers—and the spectroscopically opaque Li–O linkage.² Herein we describe a spectroscopic method used to assign β -amino ester enolates (**1**) as hexamers in solution.



To understand these studies we must briefly digress by describing the dynamic phenomena that are commonly observed for organolithium aggregates but may seem surprising to the nonspecialist.³ At the lowest attainable NMR probe temperatures (<−100 °C), fast processes including solvent exchange,⁴ conformational equilibria,⁵ and chelate isomerizations⁶ can become observable on NMR spectroscopic time scales, with concomitant spectral complexity. The spectra typically simplify on warming above −100 °C due to time averaging. Further warming of the probe often leads to a particularly odd effect in which *intra*-aggregate exchanges of ${}^6\text{Li}$ nuclei become fast, whereas *inter*-aggregate exchanges are still slow.⁷ Consequently, aggregates that differ by virtue of their aggregation numbers (dimers versus hexamers) or subunit composition (4:2 versus 3:3 mixed hexamers) appear as separate species by ${}^6\text{Li}$ NMR spectroscopy, but *each aggregate manifests a single ${}^6\text{Li}$ resonance*. This combination of rapid *intra*-aggregate exchange in conjunction with slow *inter*-aggregate exchange proves critical to the structural assignments.

The ${}^6\text{Li}$ NMR spectrum recorded on $[{}^6\text{Li}](R)\text{-1}$ in 9.0 M THF/toluene at −100 °C shows a single resonance, consistent with almost any aggregation state of high symmetry. The ${}^6\text{Li}$ NMR spectrum recorded on $[{}^6\text{Li}]rac\text{-1}$ affords a single resonance at a markedly different chemical shift than $[{}^6\text{Li}](R)\text{-1}$, suggesting the formation of a highly symmetric *heterochiral* aggregate. Partially racemic

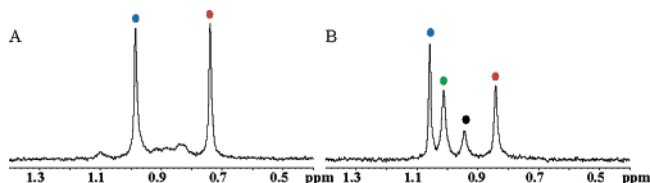


Figure 1. ${}^6\text{Li}$ NMR spectra recorded on a 0.2 M enolate mixture (50% ee) in 9.0 M THF/toluene at (A) −100 °C and (B) −50 °C: (blue) $\mathbf{R}_3\mathbf{S}_3$; (green) $\mathbf{R}_2\mathbf{S}_4/\mathbf{R}_4\mathbf{S}_2$; (black) $\mathbf{R}_1\mathbf{S}_5/\mathbf{R}_5\mathbf{S}_1$; (red) $\mathbf{R}_6\mathbf{S}_6$.

mixtures using combinations of $[{}^6\text{Li}](R)\text{-1}$ and $[{}^6\text{Li}](S)\text{-1}$ at −100 °C (Figure 1A) show both resonances along with considerable “noise” in the baseline. Additionally, ${}^6\text{Li}$ spectra recorded on $[{}^6\text{Li}, {}^{15}\text{N}](S)\text{-1}$ and $[{}^6\text{Li}, {}^{15}\text{N}]rac\text{-1}$ show ${}^6\text{Li}$ – ${}^{15}\text{N}$ coupling (d , $J_{\text{Li}-\text{N}} = 3.4$ and 3.6 Hz, respectively), confirming chelation as drawn.⁸

Varying the probe temperature from −100 to −50 °C afforded a single sharp resonance for $[{}^6\text{Li}](R)\text{-1}$, offering no evidence of latent stereoisomerism, lower symmetry, or related structural complexity. Conversely, warming samples containing varying proportions of $[{}^6\text{Li}](R)\text{-1}$ and $[{}^6\text{Li}](S)\text{-1}$ revealed *two* resonances in lieu of the baseline noise—*four* resonances in total (Figure 1B). The data are consistent with deep-seated structural complexities that simplify by rapid *intra*-aggregate exchange at elevated temperatures. Furthermore, the relative intensities are independent of the enolate concentration (0.04–0.40 M) and the THF concentration (2.0–9.0 M), indicating that the four species are at the same aggregation and solvation state.

We considered models based on homochiral aggregates (\mathbf{R}_N or \mathbf{S}_N) and heterochiral aggregates ($\mathbf{R}_n\mathbf{S}_{N-n}$). $\mathbf{R}_n\mathbf{S}_{N-n}/\mathbf{R}_{N-n}\mathbf{S}_n$ and $\mathbf{R}_N/\mathbf{S}_N$ refer to pairs of spectroscopically indistinguishable enantiomers. Dimers ($\mathbf{R}_1\mathbf{S}_1$ and $\mathbf{R}_2\mathbf{S}_2$) and tetramers ($\mathbf{R}_4\mathbf{S}_4$, $\mathbf{R}_1\mathbf{S}_3/\mathbf{R}_3\mathbf{S}_1$, and $\mathbf{R}_2\mathbf{S}_2$) afford only two and three ${}^6\text{Li}$ resonances, respectively. Conversely, four discrete resonances are consistent with an ensemble of homo- and heterochiral hexamers: $\mathbf{R}_6\mathbf{S}_6$, $\mathbf{R}_1\mathbf{S}_5/\mathbf{R}_5\mathbf{S}_1$, $\mathbf{R}_2\mathbf{S}_4/\mathbf{R}_4\mathbf{S}_2$, and $\mathbf{R}_3\mathbf{S}_3$.

A compelling picture emerges from a variant of a Job plot (Figure 2) in which the intensities of the four resonances are plotted as a function of the mole fraction of subunit (*R*)-1, X_R .⁹ The maximum observed for each aggregate coincides with the stoichiometry of the aggregate. The concentration dependencies were modeled as follows.^{10,11}

$$X_R = \frac{\sum_{n=0}^N n[\mathbf{R}_n\mathbf{S}_{N-n}]}{\sum_{n=0}^N N[\mathbf{R}_n\mathbf{S}_{N-n}]} \quad X_n = \frac{[\mathbf{R}_n\mathbf{S}_{N-n}]}{\sum_{j=0}^N [\mathbf{R}_j\mathbf{S}_{N-j}]}$$

* Department of Chemistry and Chemical Biology, Cornell University.
† Physics Department, Cornell University.
‡ Aventis.

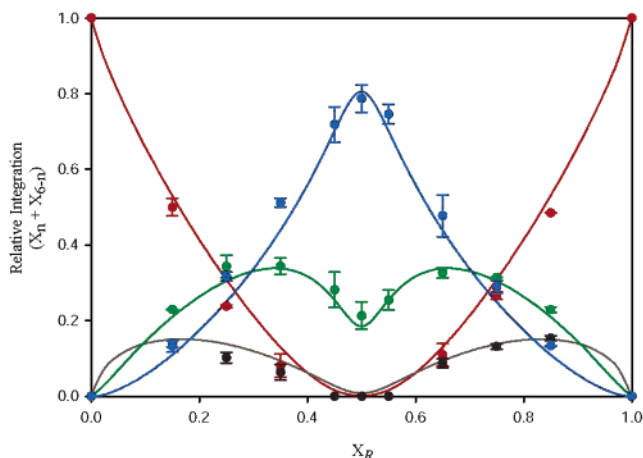


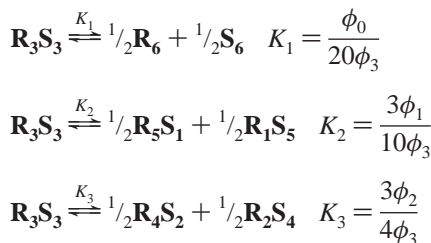
Figure 2. Job plot of the mole fraction of $\mathbf{R}_n\mathbf{S}_{6-n}/\mathbf{R}_{6-n}\mathbf{S}_n$ ($X_n + X_{6-n}$) as a function of the mole fraction of the *R* enantiomer (X_R) at -50°C . For the case where $n = 3$, only X_3 is plotted. The best fit to the data is also shown: (blue) $\mathbf{R}_3\mathbf{S}_3$; (green) $\mathbf{R}_2\mathbf{S}_4/\mathbf{R}_4\mathbf{S}_2$; (black) $\mathbf{R}_1\mathbf{S}_5/\mathbf{R}_5\mathbf{S}_1$; (red) $\mathbf{R}_6\mathbf{S}_0$.

$$[\mathbf{R}_n\mathbf{S}_{N-n}] = C \frac{N!}{n!(N-n)!} \phi_n \exp\left(\frac{n\mu_R + (N-n)\mu_S}{kT}\right)$$

where

$$\phi_n = \phi_{N-n} = \left\langle \exp\left(\frac{-g_p}{kT}\right) \right\rangle$$

X_n , the mole fraction of the aggregate, is an implicit function of X_R and ϕ_n and may be solved by an iterative parametric method. It is instructive to present the results in terms of the following equilibria:



If the aggregate distribution is purely statistical ($\phi_0 = \phi_1 = \dots = \phi_6$), then $K_1 = 0.05$, $K_2 = 0.30$, and $K_3 = 0.75$. Least-squares fits illustrated in Figure 2 yield substantially different values: $K_1 = 1.0 \pm 0.1 \times 10^{-3}$, $K_2 = 5.0 \pm 0.3 \times 10^{-3}$, and $K_3 = 115 \pm 3 \times 10^{-3}$. From the relationship $\Delta G_m = -RT \ln(K_m/K_{\text{statistical}})$, we obtain the deviations from statistical as follows: $\Delta G_1 = 1.73 \pm 0.04$ kcal/mol, $\Delta G_2 = 1.82 \pm 0.03$ kcal/mol, and $\Delta G_3 = 0.83 \pm 0.01$ kcal/mol. Therefore, the heterochiral $\mathbf{R}_3\mathbf{S}_3$ hexamer is markedly more stable than the alternative homo- and heterochiral combinations.

An X-ray crystal structure was obtained of **rac-1** showing a prismatic hexamer ($\mathbf{R}_3\mathbf{S}_3$) of S_6 symmetry (Figure 3).^{12,13} Consistent with the spectroscopic studies, this aggregate would show a single ${}^6\text{Li}$ resonance. The crystallization of the $\mathbf{R}_3\mathbf{S}_3$ form is satisfying in light of its relative stability in solution. The high stability of the $\mathbf{R}_3\mathbf{S}_3$ hexamer could influence the stereochemistry of alkylation via an asymmetric amplification.¹⁴

Detailed mechanistic studies on the alkylation of the β -amino ester enolates will be reported in due course. The spectroscopic strategy described herein may prove general for assigning structures of enolates and alkoxides. Last, we are reminded to be cautious about dismissing baseline noise.

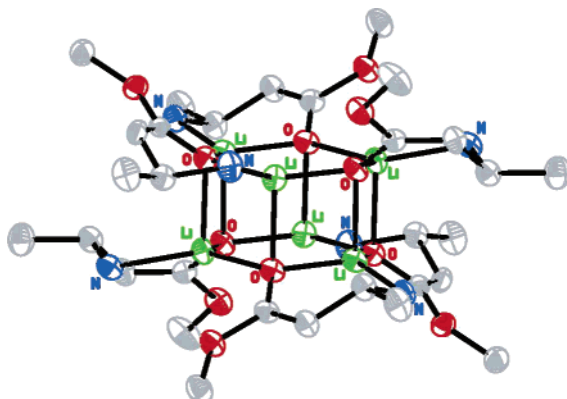


Figure 3. ORTEP of **rac-1** revealing a hexameric aggregate of S_6 symmetry. Hydrogen atoms are omitted for clarity.

Acknowledgment. We thank Prof. Benjamin Widom for helpful discussions. A.J.M. and D.B.C. thank the National Institutes of Health for direct support of this work. G.E.S.T. and S.M.G. thank the DOE for support (DE-FG02-97ER62443).

Supporting Information Available: Experimental details, spectroscopic data, mathematical derivations (PDF), and X-ray crystallographic data (CIF). This material is available free of charge via the Internet at <http://pubs.acs.org>.

References

- (1) Enolization was effected without N-lithiation using LiHMDS. Chandramouli, S. V.; O'Brien, M. K.; Powner, T. H. WO Patent 0040547, 2000. See also: Czekaj, M.; Klein, S. I.; Guertin, K. R.; Gardner, C. J.; Zulli, A. L.; Pauls, H. W.; Spada, A. P.; Cheney, D. L.; Brown, K. D.; Colussi, D. J.; Chu, V.; Leadley, R. J.; Dunwiddie, C. T. *Bioorg. Med. Chem. Lett.* **2002**, *12*, 1667–1670. Nagula, G.; Huber, V. J.; Lum, C.; Goodman, B. A. *Org. Lett.* **2000**, *2*, 3527–3529. Myers, A. G.; Gleason, J. L.; Yoon, T. *J. Am. Chem. Soc.* **1995**, *117*, 8488–8489.
- (2) Solution studies of enolate aggregation: (a) Wang, D. Z.; Streitwieser, A. *J. Org. Chem.* **2003**, *68*, 8936–8942 and references therein. (b) Jackman, L. M.; Bortiatynski, J. *Adv. Carbanion Chem.* **1992**, *1*, 45–87.
- (3) For reviews on Li NMR spectroscopy, see: Günther, H. *J. Braz. Chem. 1999*, *10*, 241–262. Günther, H. In *Advanced Applications of NMR to Organometallic Chemistry*; Gielen, M., Willem, R., Wrackmeyer, B., Eds.; Wiley & Sons: New York, 1996; pp 247–290.
- (4) For leading references, see: Lucht, B. L.; Collum, D. B. *Acc. Chem. Res.* **1999**, *32*, 1035–1042.
- (5) Remenar, J. F.; Lucht, B. L.; Kruglyak, D.; Romesberg, F. E.; Gilchrist, J. H.; Collum, D. B. *J. Org. Chem.* **1997**, *62*, 5748–5754. Collum, D. B. *Acc. Chem. Res.* **1993**, *26*, 227–234. Boche, G.; Fraenkel, G.; Cabral, J.; Harms, K.; van Eikema Hommes, N. J. R.; Lohrenz, J.; Marsch, M.; Schleyer, P. v. R. *J. Am. Chem. Soc.* **1992**, *114*, 1562–1565.
- (6) (a) Reich, H. J.; Goldenberg, W. S.; Sanders, A. W.; Jantzi, K. L.; Tschucke, C. C. *J. Am. Chem. Soc.* **2003**, *125*, 3509–3521 and references therein. (b) Aubrecht, K. B.; Lucht, B. L.; Collum, D. B. *Organometallics* **1999**, *18*, 2911–2978.
- (7) Bauer, W.; Griesinger, C. *J. Am. Chem. Soc.* **1993**, *115*, 10871–10882. See also ref 6b.
- (8) [${}^{15}\text{N}$]S-1 and [${}^{15}\text{N}$]rac-1 were synthesized via the Arndt-Eistert homologation: Podlech, J.; Seebach, D. *Liebigs Ann.* **1995**, 1217–1228.
- (9) Job, P. *Ann. Chim.* **1928**, *9*, 113–203. Gil, V. M. S.; Oliveira, N. C. *J. Chem. Educ.* **1990**, *67*, 473–478.
- (10) Widom, B. *Statistical Mechanics: A Concise Introduction for Chemists*; Cambridge University Press: New York, 2002.
- (11) Where μ_R and μ_S are the chemical potentials of *R* and *S*, g_p corresponds to the free energy of assembly for each permutation, and C is a constant.
- (12) **rac-1** (0.20 M) was crystallized from a 9.0 M THF/toluene solution held at -20°C over 24 h.
- (13) For more examples of ester enolate crystal structures, see: Williard, P. G. *Comprehensive Organic Synthesis*; Pergamon: New York, 1991; Vol. 1, pp 1–47. Seebach, D. *Angew. Chem., Int. Ed. Engl.* **1988**, *27*, 1624–1654. Boche, G.; Langlotz, I.; Marsch, M.; Harms, K. *Chem. Ber.* **1994**, *127*, 2059–2064. Jastrzebski, J. T. B. H.; van Koten, G.; van de Mieroop, W. F. *Inorg. Chim. Acta* **1988**, *142*, 169–171.
- (14) Fenwick, D. R.; Kagan, H. B. *Top. Stereochem.* **1999**, *22*, 257–296.

JA049245S

Characterization of β -Amino Ester Enolates as Hexamers via ^6Li NMR Spectroscopy

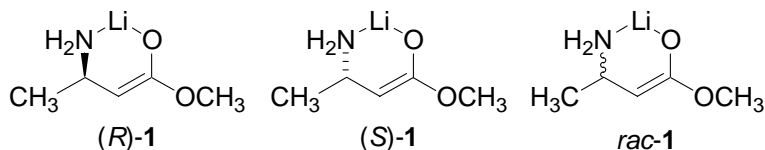
Anne J. McNeil,[†] Gilman E. S. Toombes,[‡] Sithamalli V. Chandramouli,[§] Benoit J. Vanasse,[§] Timothy A. Ayers,[§] Michael K. O'Brien,[§] Emil Lobkovsky,[†] Sol M. Gruner,[‡] John A. Marohn,[†] and David B. Collum^{*,‡}

[†]Department of Chemistry and Chemical Biology, Baker Laboratory, Cornell University, Ithaca, New York 14853-1301

[‡]Physics Department, Clark Hall, Cornell University, Ithaca, New York 14853-2501

[§]Aventis, Process Development Chemistry, Bridgewater, New Jersey, 08807

Supporting Information



NMR Structural Studies

- I. ^6Li NMR Spectra recorded on $[^6\text{Li}](R)\text{-1}$, $[^6\text{Li}, ^{15}\text{N}](S)\text{-1}$, $[^6\text{Li}]rac\text{-1}$, and $[^6\text{Li}, ^{15}\text{N}]rac\text{-1}$ in 9.8 M THF/cyclopentane at -90 °C.
- II. ^6Li NMR Spectra recorded on $[^6\text{Li}](R)\text{-1}$ (0.20 M) in 9.0 M THF/toluene at various temperatures.
- III. ^6Li NMR Spectra recorded on $[^6\text{Li}]rac\text{-1}$ (0.20 M) in 9.0 M THF/toluene at various temperatures.
- IV. ^6Li NMR Spectra recorded on a mixture of $[^6\text{Li}](R)\text{-1}$ (0.10 M) and $[^6\text{Li}]rac\text{-1}$ (0.10 M) in 9.0 M THF/toluene at various temperatures.
- V. ^6Li NMR Spectra recorded on a mixture of $[^6\text{Li}](R)\text{-1}$ and $[^6\text{Li}]rac\text{-1}$ (50 % ee) in 9.0 M THF/toluene at -50 °C at various enolate concentrations.
- VI. Plot of the mole fraction of the aggregate ($X_n + X_{6-n}$) versus [enolate] for the spectra in section V.
- VII. Table of data for the plot in section VI.
- VIII. ^6Li NMR Spectra recorded on a mixture of $[^6\text{Li}](R)\text{-1}$ and $[^6\text{Li}]rac\text{-1}$ (50 % ee) at -50 °C in various THF concentrations (toluene co-solvent).
- IX. Plot of the mole fraction of the aggregate ($X_n + X_{6-n}$) versus [THF] for the spectra in section VIII.
- X. Table of data for the plot in section IX.

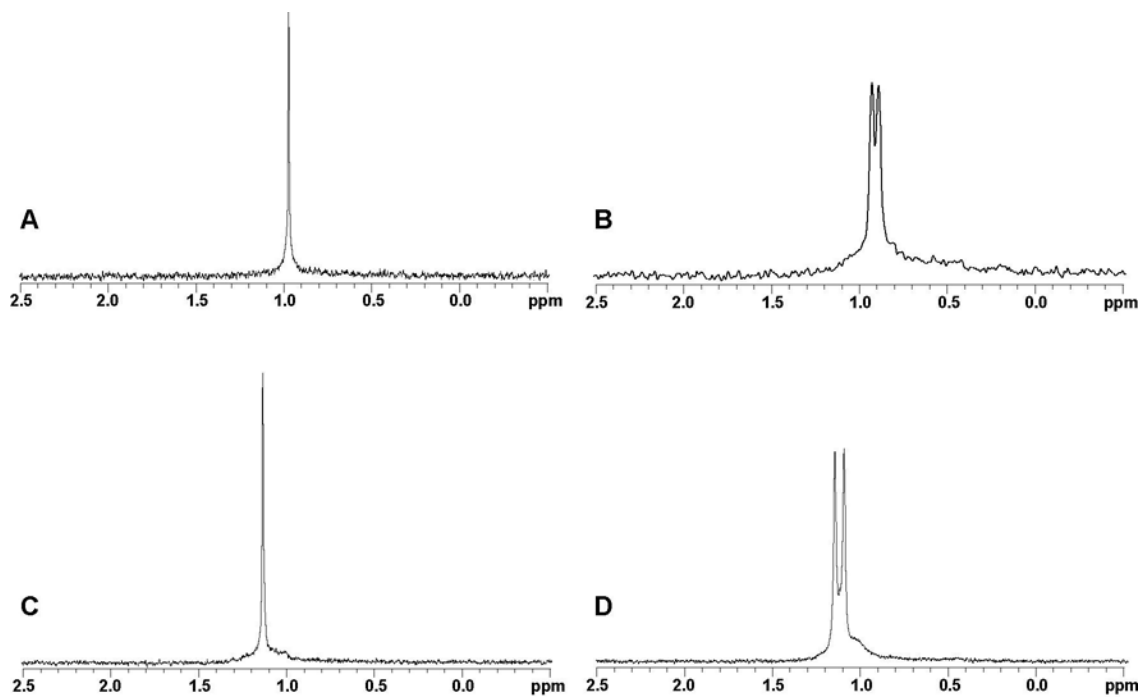
- XI.** ^6Li NMR Spectra recorded on mixtures of [$^6\text{Li}(S)$]-**1** and [$^6\text{Li}]\text{rac-1}$ at -50 °C in 9.0 M THF/toluene.
- XII.** ^6Li NMR Spectra recorded on mixtures of [$^6\text{Li}(R)$]-**1** and [$^6\text{Li}]\text{rac-1}$ at -50 °C in 9.0 M THF/toluene.
- XIII.** Plot of the mole fraction of the aggregate ($X_n + X_{6-n}$) versus the mole fraction of *R* (X_R) for the spectra in sections **XI** and **XII**.
- XIV.** Table of data for the plot in section **XIII**.

Mathematical Derivations

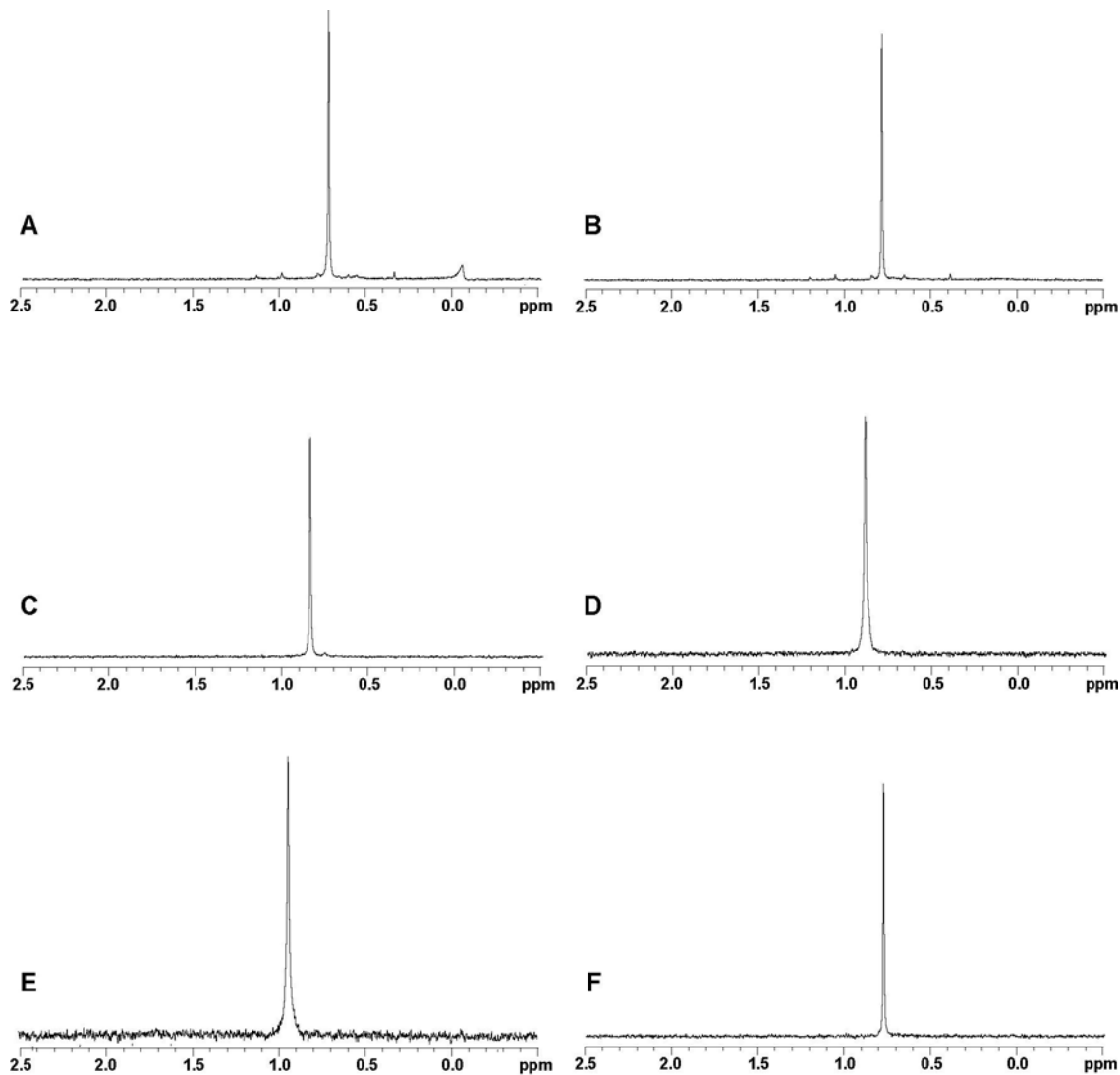
- I.** Introduction to the model.
- II.** Boltzmann distribution.
- III.** Multiplicity.
- IV.** Chemical potential.
- V.** The statistical case.
- VI.** The parametric method.
- VII.** Fitting the experimental data with the parametric method.
- VIII.** Equilibrium constants.

Crystal Structure Data

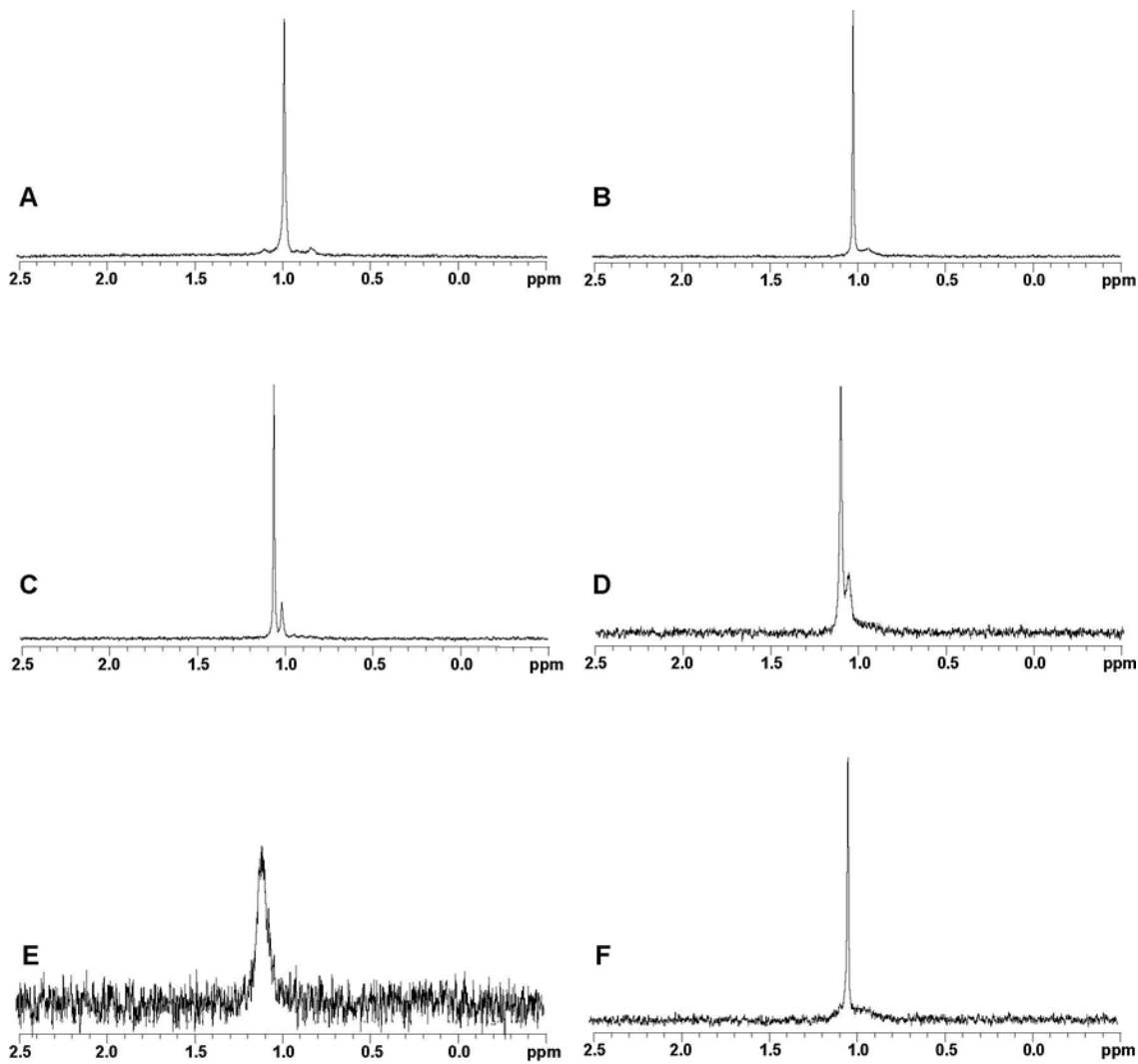
- I.** Crystal structure: ORTEP.
- II.** Crystal data and structure refinement.
- III.** Table of bond lengths and angles.



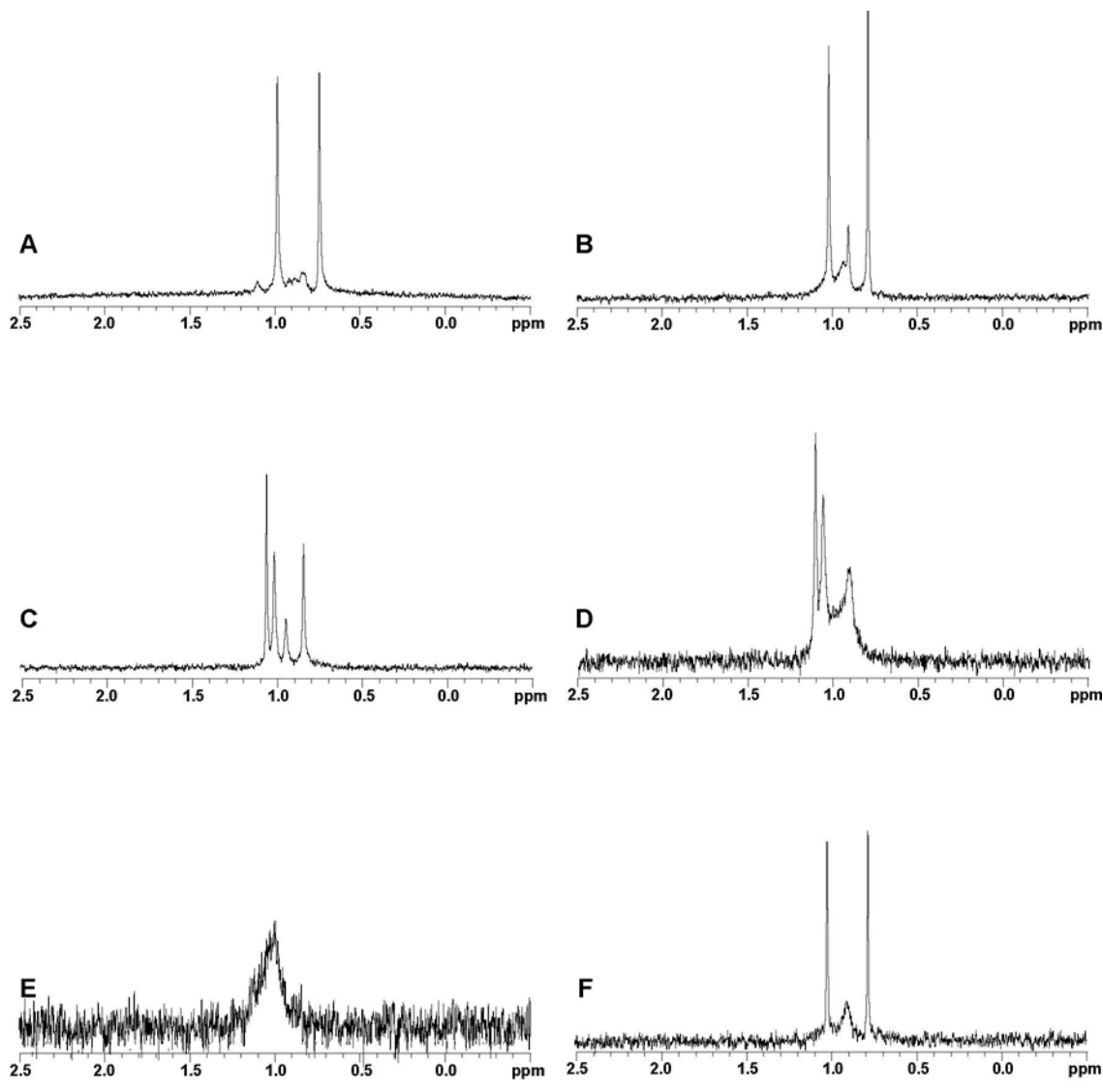
I. ${}^6\text{Li}$ NMR Spectra recorded in 9.8 M THF/cyclopentane at -90 °C: (A) $[{}^6\text{Li}](R)\text{-1}$ (0.07 M); (B) $[{}^6\text{Li}, {}^{15}\text{N}](S)\text{-1}$ (0.13 M); (C) $[{}^6\text{Li}]rac\text{-1}$ (0.13 M); (D) $[{}^6\text{Li}, {}^{15}\text{N}]rac\text{-1}$ (0.33 M).



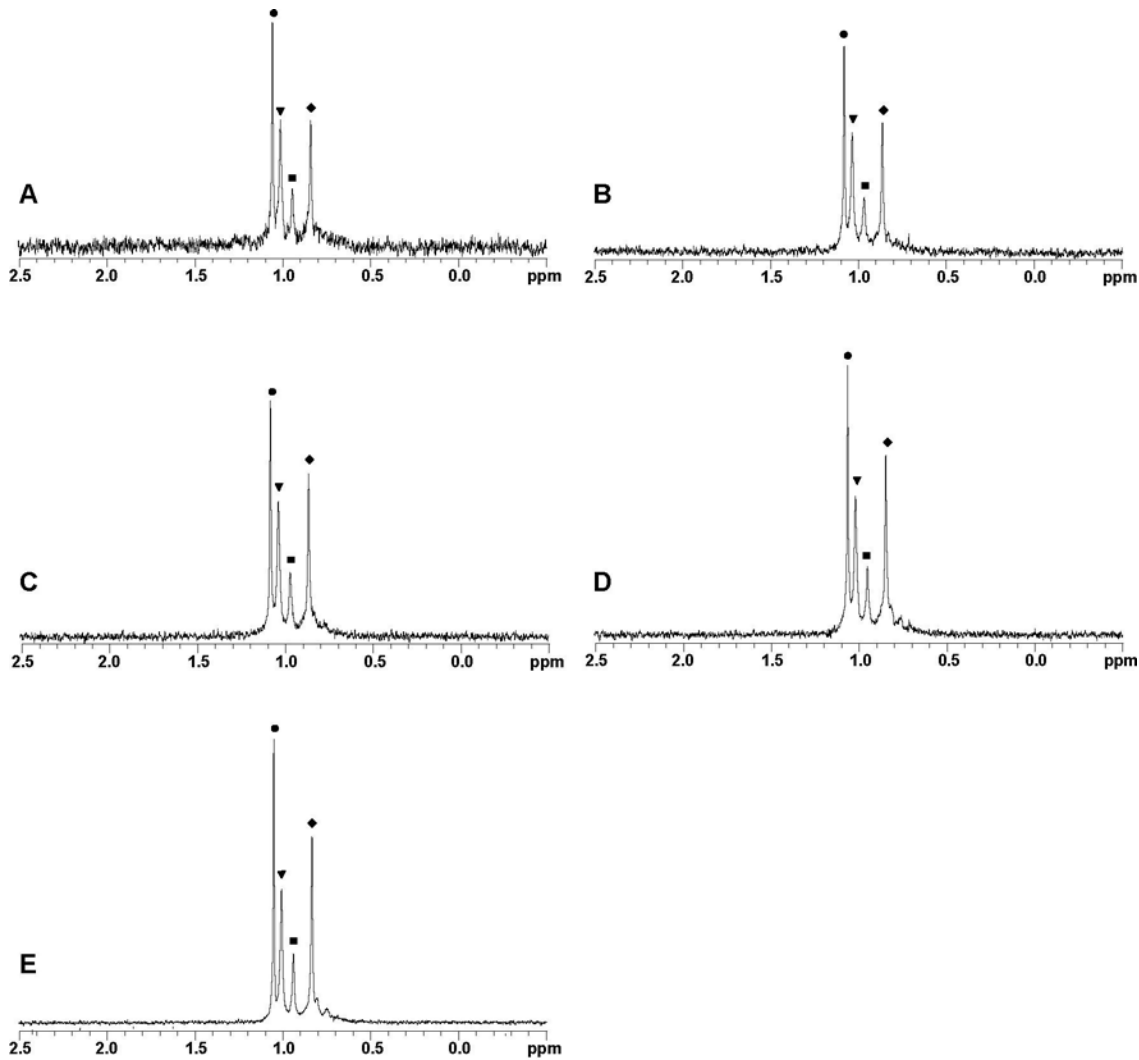
II. ${}^6\text{Li}$ NMR Spectra recorded on $[{}^6\text{Li}](R)\text{-1}$ (0.20 M) in 9.0 M THF/toluene: (A) -100 $^\circ\text{C}$; (B) -75 $^\circ\text{C}$; (C) -50 $^\circ\text{C}$; (D) -25 $^\circ\text{C}$; (E) 0 $^\circ\text{C}$; (F) -90 $^\circ\text{C}$ after temperature series.



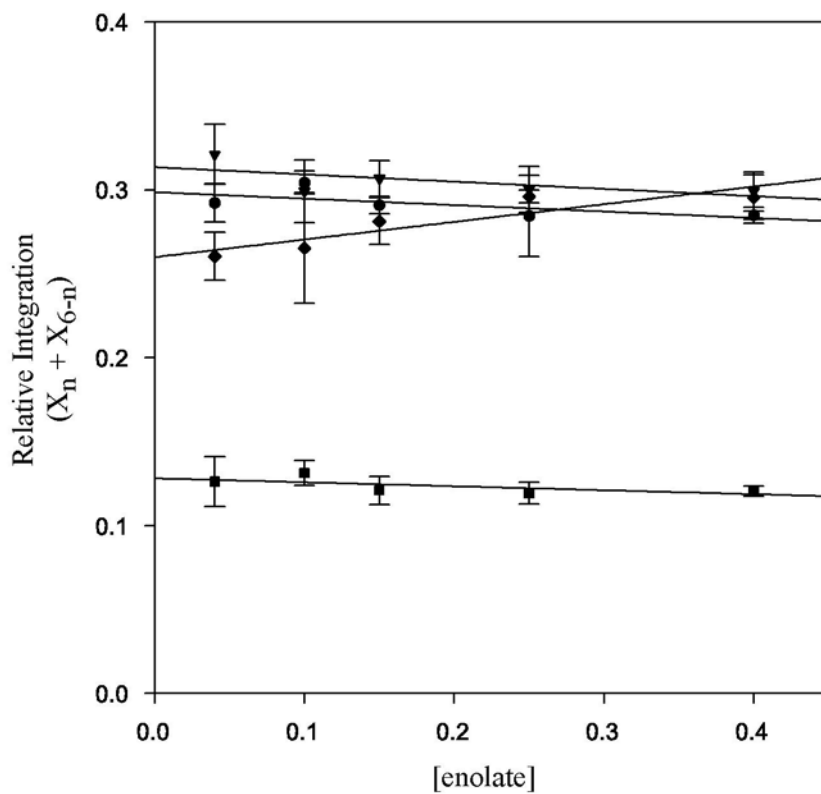
III. ${}^6\text{Li}$ NMR Spectra recorded on $[{}^6\text{Li}]\text{rac-1}$ (0.20 M) in 9.0 M THF/toluene: (A) -100 °C; (B) -75 °C; (C) -50 °C; (D) -25 °C; (E) 0 °C; (F) -90 °C after temperature series.



IV. ${}^6\text{Li}$ NMR Spectra recorded on a mixture of $[{}^6\text{Li}](R)\text{-1}$ (0.10 M) and $[{}^6\text{Li}]rac\text{-1}$ (0.10 M) in 9.0 M THF/toluene: (A) -100 °C; (B) -75 °C; (C) -50 °C; (D) -25 °C; (E) 0 °C; (F) -90 °C after temperature series.



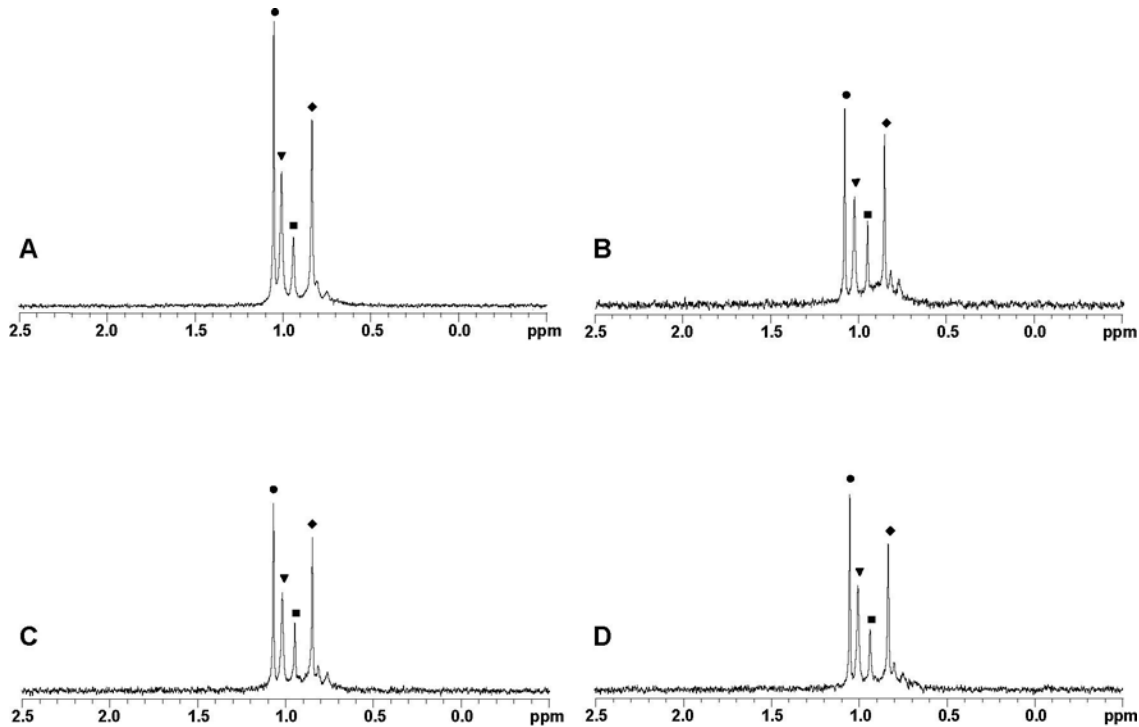
V. ${}^6\text{Li}$ NMR Spectra recorded on a mixture of $[{}^6\text{Li}](R)\text{-1}$ and $[{}^6\text{Li}]rac\text{-1}$ (50 % ee) in 9.0 M THF/toluene at -50 °C at various enolate concentrations: (A) 0.04 M; (B) 0.10 M; (C) 0.15 M; (D) 0.25 M; (E) 0.40 M. (\bullet) R_3S_3 ; (∇) $\text{R}_4\text{S}_2/\text{R}_2\text{S}_4$; (\blacksquare) $\text{R}_5\text{S}_1/\text{R}_1\text{S}_5$; (\blacklozenge) R_6/S_6 . $\text{R}_n\text{S}_{\text{N}-n}/\text{R}_{\text{N}-n}\text{S}_n$ and R_N/S_N refer to pairs of spectroscopically indistinguishable enantiomers.



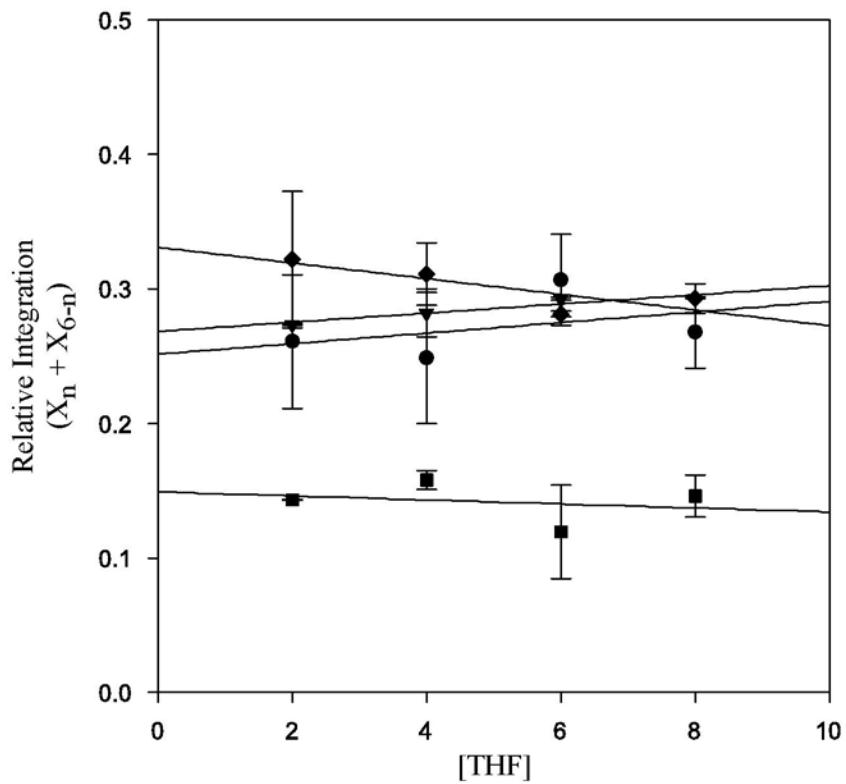
VI. Plot of the mole fraction of the aggregate ($X_n + X_{6-n}$) versus [enolate] for the spectra in section V. For the case where $n = 3$, only X_3 is plotted. (●) $\mathbf{R}_3\mathbf{S}_3$; (▼) $\mathbf{R}_4\mathbf{S}_2/\mathbf{R}_2\mathbf{S}_4$; (■) $\mathbf{R}_5\mathbf{S}_1/\mathbf{R}_1\mathbf{S}_5$; (◆) $\mathbf{R}_6/\mathbf{S}_6$.

VII. Table of data for the plot in section VI. ($[^6\text{Li}](R)\text{-1}$ and $[^6\text{Li}]rac\text{-1}$ (50 % ee) in 9.0 M THF/toluene at -50 °C.)

[enolate] (M)	$\mathbf{R}_3\mathbf{S}_3$	$\mathbf{R}_4\mathbf{S}_2/\mathbf{R}_2\mathbf{S}_4$	$\mathbf{R}_5\mathbf{S}_1/\mathbf{R}_1\mathbf{S}_5$	$\mathbf{R}_6/\mathbf{S}_6$
0.04	0.29 ± 0.01	0.32 ± 0.02	0.13 ± 0.01	0.26 ± 0.01
0.10	0.30 ± 0.01	0.30 ± 0.02	0.13 ± 0.01	0.27 ± 0.03
0.15	0.29 ± 0.01	0.31 ± 0.01	0.12 ± 0.01	0.28 ± 0.01
0.25	0.28 ± 0.02	0.30 ± 0.01	0.12 ± 0.01	0.296 ± 0.004
0.40	0.285 ± 0.002	0.30 ± 0.01	0.120 ± 0.003	0.30 ± 0.02



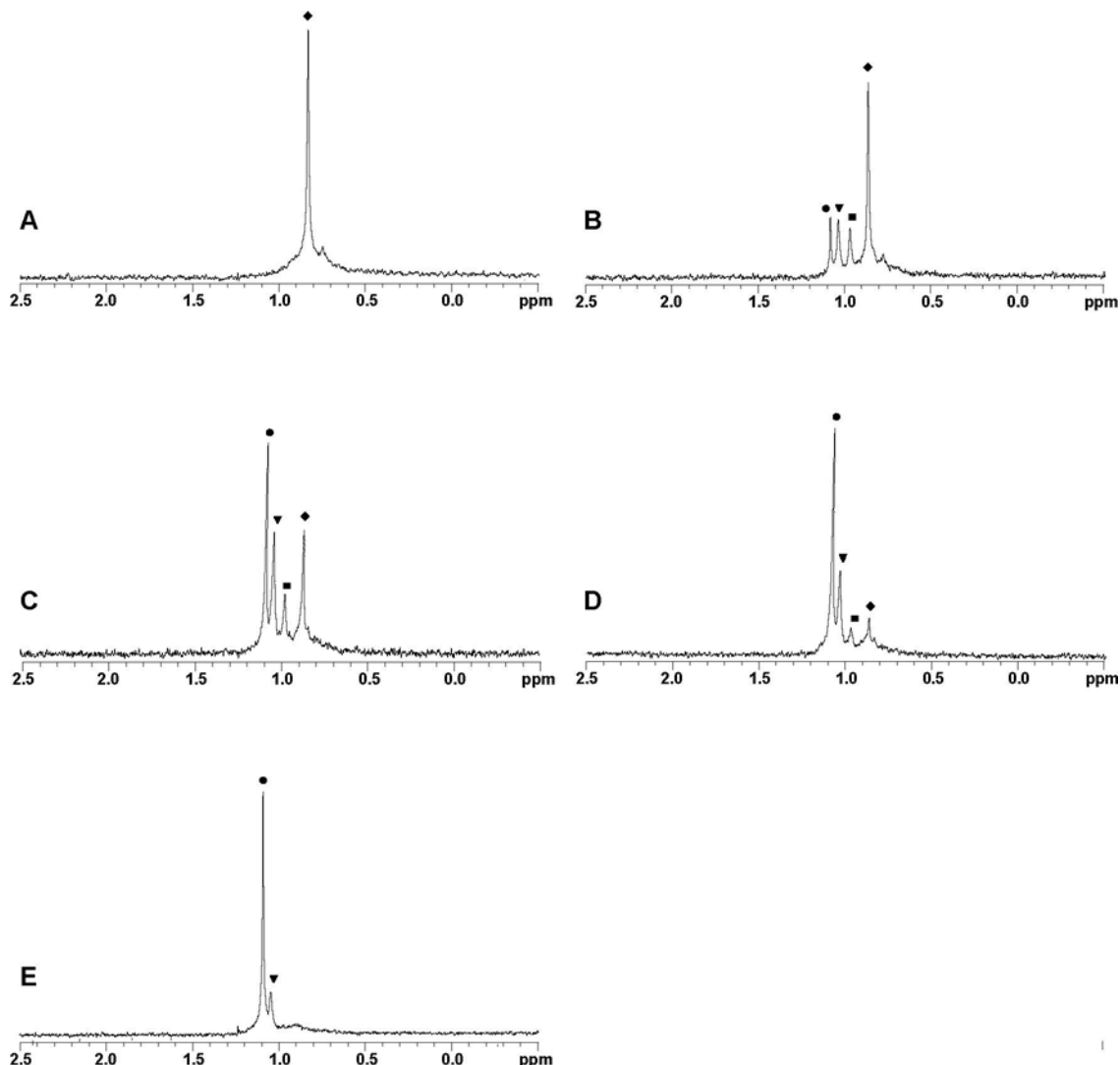
VIII. ${}^6\text{Li}$ NMR Spectra recorded on a mixture of $[{}^6\text{Li}](R)\text{-1}$ and $[{}^6\text{Li}]rac\text{-1}$ (50 % ee) in various THF concentrations (toluene co-solvent) at -50 °C: (A) 2.0 M; (B) 4.0 M; (C) 6.0 M; (D) 8.0 M.
 (●) R_3S_3 ; (▼) $\text{R}_4\text{S}_2/\text{R}_2\text{S}_4$; (■) $\text{R}_5\text{S}_1/\text{R}_1\text{S}_5$; (◆) R_6S_6 .



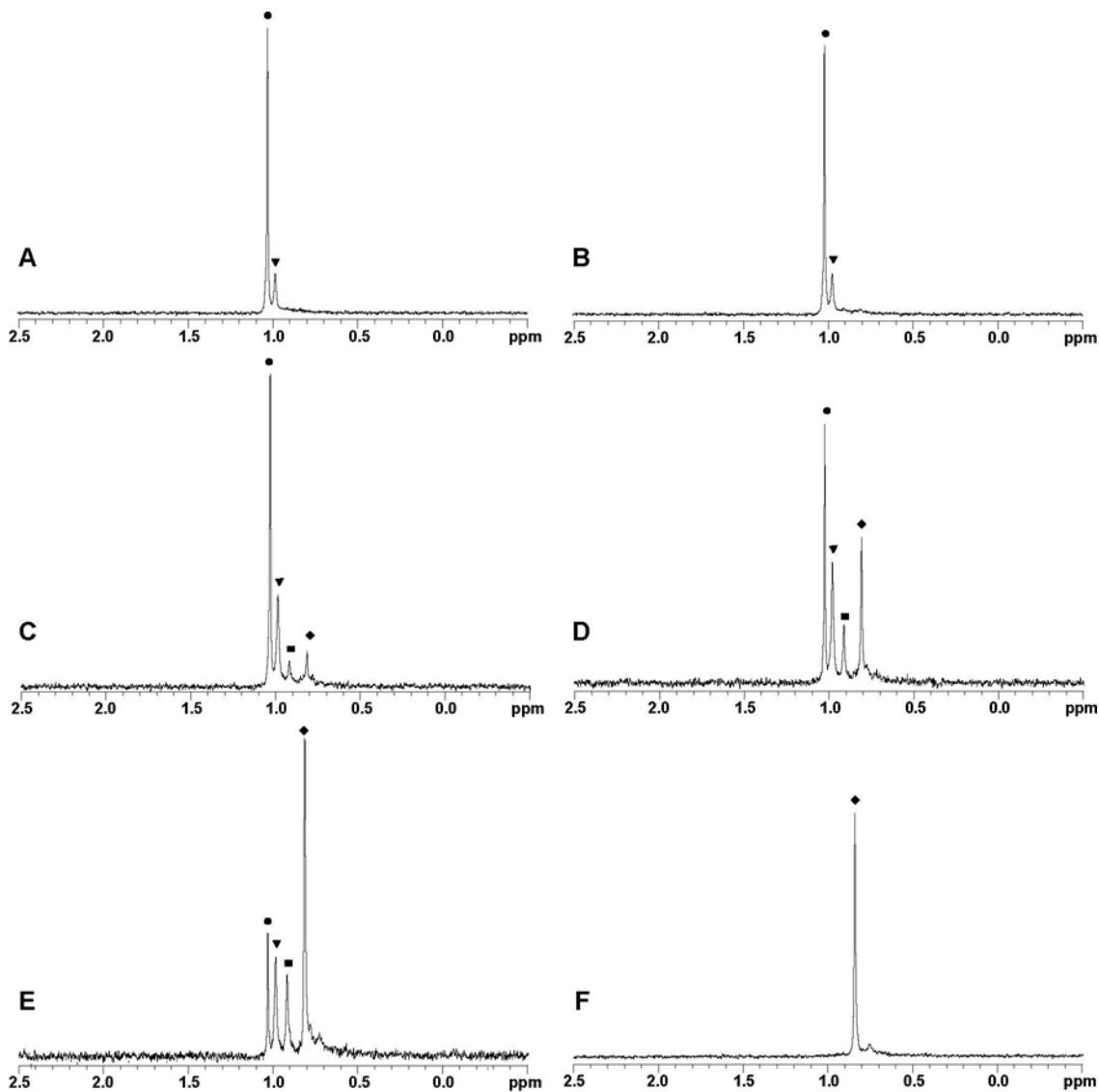
IX. Plot of the mole fraction of the aggregate ($X_n + X_{6-n}$) versus [THF] for the spectra in section **VIII**. For the case where $n = 3$, only X_3 is plotted. (●) $\mathbf{R}_3\mathbf{S}_3$; (▼) $\mathbf{R}_4\mathbf{S}_2/\mathbf{R}_2\mathbf{S}_4$; (■) $\mathbf{R}_5\mathbf{S}_1/\mathbf{R}_1\mathbf{S}_5$; (◆) $\mathbf{R}_6/\mathbf{S}_6$.

X. Table of data for the plot in section **IX**. ($[{}^6\text{Li}](R)\text{-1}$ and $[{}^6\text{Li}]rac\text{-1}$ (50 %ee) in various THF concentrations (toluene co-solvent) at -50 °C.)

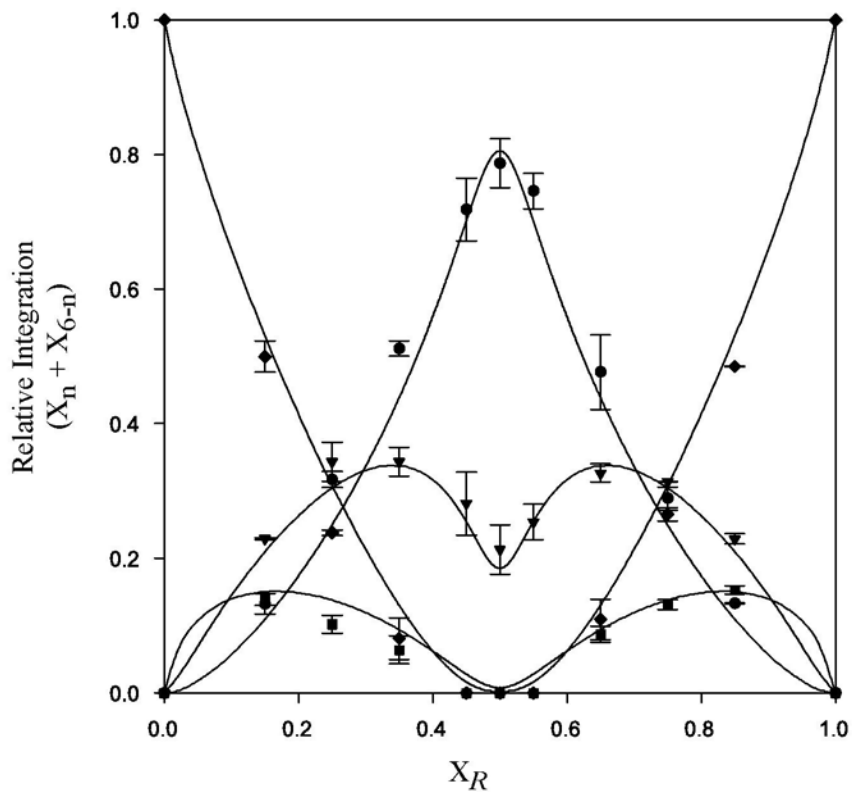
[THF] (M)	$\mathbf{R}_3\mathbf{S}_3$	$\mathbf{R}_4\mathbf{S}_2/\mathbf{R}_2\mathbf{S}_4$	$\mathbf{R}_5\mathbf{S}_1/\mathbf{R}_1\mathbf{S}_5$	$\mathbf{R}_6/\mathbf{S}_6$
2.0	0.26 ± 0.05	0.274 ± 0.001	0.143 ± 0.001	0.32 ± 0.05
4.0	0.25 ± 0.05	0.28 ± 0.02	0.16 ± 0.01	0.31 ± 0.02
6.0	0.31 ± 0.03	0.293 ± 0.001	0.12 ± 0.03	0.281 ± 0.002
8.0	0.27 ± 0.03	0.293 ± 0.001	0.15 ± 0.02	0.29 ± 0.01



XI. ${}^6\text{Li}$ NMR Spectra recorded on mixtures of $[{}^6\text{Li}](S)\text{-1}$ and $[{}^6\text{Li}]rac\text{-1}$ ($[\text{enolate}]_{\text{total}} = 0.10 \text{ M}$) at -50°C in 9.0 M THF/toluene: (A) $X_R = 0.0$; (B) $X_R = 0.15$; (C) $X_R = 0.25$; (D) $X_R = 0.35$; (E) $X_R = 0.45$. (●) $\mathbf{R}_3\mathbf{S}_3$; (▼) $\mathbf{R}_4\mathbf{S}_2/\mathbf{R}_2\mathbf{S}_4$; (■) $\mathbf{R}_5\mathbf{S}_1/\mathbf{R}_1\mathbf{S}_5$; (◆) $\mathbf{R}_6/\mathbf{S}_6$.



XII. ^6Li NMR Spectra recorded on mixtures of $[^6\text{Li}](R)\text{-1}$ and $[^6\text{Li}]rac\text{-1}$ ($[\text{enolate}]_{\text{total}} = 0.10 \text{ M}$) at -50°C in 9.0 M THF/toluene: (A) $X_R = 0.50$; (B) $X_R = 0.55$; (C) $X_R = 0.65$; (D) $X_R = 0.75$; (E) $X_R = 0.85$; (F) $X_R = 1.0$. (●) R_3S_3 ; (▼) $\text{R}_4\text{S}_2/\text{R}_2\text{S}_4$; (■) $\text{R}_5\text{S}_1/\text{R}_1\text{S}_5$; (◆) R_6S_6 .



XIII. Plot of the mole fraction of the aggregate ($X_n + X_{6-n}$) versus the mole fraction of R (X_R) for the spectra in sections **XI** and **XII**. For the case where $n = 3$, only X_3 is plotted. (●) $\mathbf{R}_3\mathbf{S}_3$; (▼) $\mathbf{R}_4\mathbf{S}_2/\mathbf{R}_2\mathbf{S}_4$; (■) $\mathbf{R}_5\mathbf{S}_1/\mathbf{R}_1\mathbf{S}_5$; (◆) $\mathbf{R}_6/\mathbf{S}_6$. See “Mathematical Derivations” section **VII** for details of the fit.

XIV. Table of data for the plot in section **XIII**. (0.10 M [enolate]_{total} at -50 °C in 9.0 M THF/toluene.)

X_R	$\mathbf{R}_3\mathbf{S}_3$	$\mathbf{R}_4\mathbf{S}_2/\mathbf{R}_2\mathbf{S}_4$	$\mathbf{R}_5\mathbf{S}_1/\mathbf{R}_1\mathbf{S}_5$	$\mathbf{R}_6/\mathbf{S}_6$
0.00	0.00 ± 0.00	0.00 ± 0.00	0.00 ± 0.00	1.00 ± 0.00
0.15	0.13 ± 0.02	0.230 ± 0.001	0.14 ± 0.01	0.50 ± 0.02
0.25	0.32 ± 0.01	0.34 ± 0.03	0.10 ± 0.01	0.238 ± 0.003
0.35	0.51 ± 0.01	0.34 ± 0.02	0.06 ± 0.02	0.08 ± 0.03
0.40	0.72 ± 0.05	0.28 ± 0.05	0.00 ± 0.00	0.00 ± 0.00
0.50	0.79 ± 0.04	0.21 ± 0.04	0.00 ± 0.00	0.00 ± 0.00
0.55	0.75 ± 0.03	0.25 ± 0.03	0.00 ± 0.00	0.00 ± 0.00
0.65	0.48 ± 0.06	0.33 ± 0.01	0.09 ± 0.01	0.11 ± 0.03
0.75	0.29 ± 0.02	0.314 ± 0.001	0.13 ± 0.01	0.27 ± 0.01
0.85	0.133 ± 0.001	0.23 ± 0.01	0.15 ± 0.01	0.485 ± 0.001
1.00	0.00 ± 0.00	0.00 ± 0.00	0.00 ± 0.00	1.00 ± 0.00

Mathematical Derivations

I. Introduction: We consider a situation where the two enantiomers, (*R*)-1 and (*S*)-1, assemble in solution to form hexamers ($N = 6$). For an individual hexamer, each of the six positions in the assembly can be occupied by an (*R*)-1 or an (*S*)-1 (hereafter denoted as R and S, respectively). One way to describe a hexamer is by listing the occupant of each position – RSSRSR, RRRRRR, or RSSSRS for example. Rather than consider the concentration of each permutation, P , we can group them according to the number of R subunits in the hexamer, n_p . The concentration, $[R_n S_{N-n}]$, of states for which $n_p = n$ is given by the Boltzmann distribution. It will depend on

1. Multiplicity (M_n) : The number of permutations of P for which $n_p = n$. By example, RSRSRS and SRRSSR are just two of 20 permutations with $n_p = 3$.
2. Free Energy (g_p) : Each permutation may have a different energy of assembly/association. For example, RRRSSS may be a much less stable permutation than RSRSRS.
3. Chemical Potential (μ_R and μ_S) : The total amount of R, $[R_{\text{total}}]$, and S, $[S_{\text{total}}]$, will set the chemical potentials and shift the likelihood of various states. If $[R_{\text{total}}] \gg [S_{\text{total}}]$, for instance, then the $[R_1 S_5]$ will be much less likely than $[R_5 S_1]$.

In the experiment, the independent variable is the mole fraction of subunits of R, X_R , and the dependent variables are linear combinations of the mole fraction of $[R_n S_{N-n}]$, X_n . Thus, we wish to predict X_n as a function of X_R for a given model.

In Section **II** we use the Boltzmann distribution to give the value of $[R_n S_{N-n}]$ in terms of free energies, multiplicity and chemical potential. In Section **III** we give an explicit form for the multiplicity. The relationship between chemical potentials and $[R_{\text{total}}]$, $[S_{\text{total}}]$ (or X_R and X_S) is derived in Section **IV**.

Section **V** considers the case where the free energies of assembly for all the permutations are equal (statistical case) for which a simple analytic result is possible. As there are no model parameters in the statistical case, the data either fits the model or the statistical assumption is invalid.

The general case does not have a simple analytic solution. A parametric approach is described in Section **VI**. This numeric method allows one to compare the experimental and predicted populations, X_n , for a given set of free energies. We obtain the residual error after an iterative optimization of the free energies to fit the data, thus giving a measure of the model's validity. Section **VII** describes the implementation of this approach. Section **VIII** relates free energies to equilibrium constants within the system.

II. Boltzmann Distribution: Consider a given permutation, P, with n_p subunits of type R and $N-n_p$ monomers of type S. The Boltzmann distribution gives its equilibrium concentration as

$$[P] = C \times \exp\left(\frac{-g_P + n_p \mu_R + (N - n_p) \mu_S}{kT}\right)$$

where C is a constant, g_P is the free energy of assembly of P, μ_R is the chemical potential of R and μ_S is the chemical potential of S (Widom, B. *Statistical Mechanics: A Concise Introduction for Chemists*; Cambridge University Press: New York, 2002). Within the experiment, all states for which $n_p = n$ are indistinguishable. The concentration of permutations for which $n_p = n$ is given by

$$\begin{aligned} [R_n S_{N-n}] &= \sum_{P; n_p=n} [P] = C \times \exp\left(\frac{n\mu_R + (N - n)\mu_S}{kT}\right) \times \sum_{P; n_p=n} \exp\left(\frac{-g_P}{kT}\right) \\ &= C \times \exp\left(\frac{n\mu_R + (N - n)\mu_S}{kT}\right) \times M_n \times \left\langle \exp\left(\frac{-g_P}{kT}\right) \right\rangle_{P; n_p=n} \end{aligned}$$

where M_n is the multiplicity (number of permutations P where $n_p = n$) and the average of free energy is taken over all states for which $n_p = n$. It will be helpful for the remainder of the discussion to define some “effective” variables

$$r = \exp\left(\frac{\mu_R}{kT}\right) \quad s = \exp\left(\frac{\mu_S}{kT}\right) \quad \phi_n = \left\langle \exp\left(\frac{-g_P}{kT}\right) \right\rangle_{P; n_p=n}$$

Substituting these into the above expression gives

$$[R_n S_{N-n}] = C \times M_n \times \phi_n \times r^n \times s^{N-n} \quad (1)$$

Increasing the chemical potential of R increases the value of “r” and favors the $[R_6S_0]$, $[R_5S_1]$, etc. states. Increasing the chemical potential of S increases the value of “s” which then favors $[R_0S_6]$, $[R_1S_5]$, etc.

ϕ_n describes the mean free energy of permutations in $[R_n S_{N-n}]$. Increasing ϕ_n favors $[R_n S_{N-n}]$ as would be expected if those states have a low free energy. Not all values of ϕ_n are independent. The free energy of a permutation, P, and the free energy of one in which R and S have been exchanged are the same because the aggregates are enantiomers. This has the important consequence that

$$\phi_n = \phi_{N-n}$$

Furthermore, free energies can only be measured relative to the free energy of a reference state. For example, if free energies are measured relative to that of $[R_6S_0]$ then $\phi_0 = \phi_6 = 1$. When N is even, $N/2$ of the values of ϕ_n are independent. For example, when $N = 6$, ϕ_1, ϕ_2 , and ϕ_3 are independent of each other.

III. Multiplicity: The value of M_n can be directly obtained by an exhaustive grouping of all hexamer permutations.

Species	n	M_n - Number of permutations	Permutations
R_0S_6	0	1	SSSSSS
R_1S_5	1	6	RSSSSS, SRSSSS, SSRSSS, SSSRSS, SSSSRS, SSSSSR
R_2S_4	2	15	RRSSSS, RSRSSS, RSSRSS, RSSRS, RSSSSR, SRRSSS, SRSRSS, SRSSRS, SRSSSR, SSRRSS, SSRSSRS, SSRSSR, SSSRRS, SSSRSR, SSSSRR
R_3S_3	3	20	RRRSSS, RRSRSS, RRSSRS, RRSSSR, RSRRSS, RSRSRS, RSRSSR, RSSRRS, RSSRSR, RSSSSR, + 10 other states with R and S switched
R_4S_2	4	15	SSRRRR, SRSRRR, SRRSRR, SRRRSR, SRRRRS, RSSRRR, RSRSRR, RSRRSR, RSRRRS, RRSSRR, RRSRSR, RRSRRS, RRRSSR, RRRSRS, RRRRSS
R_5S_1	5	6	SRRRRR, RSRRRR, RRSRRR, RRRSRR, RRRRSR, RRRRRS
R_6S_0	6	1	RRRRRR

Alternatively, one can use Pascal's triangle or the binomial theorem to achieve the general result

$$\text{Multiplicity} = M_n = \frac{N!}{(N-n)! \times n!}.$$

IV. Chemical Potential: The experimental variables are the mole fractions of $[R_n S_{N-n}]$, X_n , and the mole fraction of R, X_R . Their relationships to C, r and s are described below.

Using eq 1 to compute $[R_n S_{N-n}]$, the mole fraction X_n is given by

$$X_n = \frac{[R_n S_{N-n}]}{\sum_{j=0}^N [R_j S_{N-j}]} = \frac{C \times M_n \times \phi_n \times r^n \times s^{N-n}}{\sum_{j=0}^N C \times M_j \times \phi_j \times r^j \times s^{N-j}} = \frac{M_n \times \phi_n \times \left(\frac{r}{s}\right)^n}{\sum_{j=0}^N M_j \times \phi_j \times \left(\frac{r}{s}\right)^j} \quad (2)$$

$$= \frac{M_n \times \phi_n \times \exp\left(\frac{n \times (\mu_R - \mu_S)}{kT}\right)}{\sum_{j=0}^N M_j \times \phi_j \times \exp\left(\frac{j \times (\mu_R - \mu_S)}{kT}\right)}$$

which is independent of the value of C.

Permutations with $[R_n S_{N-n}]$ contain n subunits of R and N-n subunits of S. Thus, the mole fraction of R, X_R , is given by

$$X_R = \frac{[R]_{total}}{[R]_{total} + [S]_{total}} = \frac{\sum_{n=0}^N n \times [R_n S_{N-n}]}{\sum_{n=0}^N N \times [R_n S_{N-n}]} \quad (3)$$

$$= \frac{\sum_{n=0}^N n \times M_n \times \phi_n \times r^n \times s^{N-n}}{\sum_{n=0}^N N \times M_n \times \phi_n \times r^n \times s^{N-n}} = \frac{\sum_{n=0}^N n \times M_n \times \phi_n \times \left(\frac{r}{s}\right)^n}{\sum_{n=0}^N N \times M_n \times \phi_n \times \left(\frac{r}{s}\right)^n}$$

All mole fractions depend only on the ratio r/s and ϕ_n , and X_R is a strictly monotonic function of r/s . Thus, if the mole fraction, X_R , and ϕ_n are known, eq 3 uniquely determines r/s . Knowing r/s , the value of any mole fraction, X_n , can be computed using eq 2.

In the special “statistical” case there is a simple analytic form for r/s . This case is examined in Section V. For the general case, r/s is most easily determined numerically. A parametric approach is described in Sections VI and VII.

V. The Statistical Case: Eq 3 can be considerably simplified if every permutation (RRSRRS, SRRRRR, etc.) has the same free energy. In this case, ϕ_n is independent of n so eq 3 simplifies to

$$\begin{aligned} X_R &= \frac{\sum_{n=0}^N n M_n \phi_n r^n s^{N-n}}{\sum_{n=0}^N N M_n \phi_n r^n s^{N-n}} = \frac{\sum_{n=0}^N n M_n r^n s^{N-n}}{\sum_{n=0}^N N M_n r^n s^{N-n}} \\ &= \frac{\sum_{n=0}^N n \times \frac{N!}{n!(N-n)!} \times r^n \times s^{N-n}}{\sum_{n=0}^N N \times \frac{N!}{n!(N-n)!} \times r^n \times s^{N-n}} \end{aligned}$$

Using the Binomial expansion

$$\sum_{j=0}^N \frac{N!}{j!(N-j)!} a^j b^{N-j} = (a+b)^N$$

gives

$$X_R = \frac{N \times r \times (r+s)^{N-1}}{N \times (r+s)^N} = \frac{r}{r+s} \leftrightarrow \frac{r}{s} = \frac{X_R}{1-X_R} \quad (4)$$

which is an explicit expression for r/s as a function of X_R . Substituting eq 4 into eq 2 determines the concentration of any species in solution in terms of X_R . The mole fraction of $[R_n S_{N-n}]$, X_n , is equal to

$$\begin{aligned} X_n &= \frac{M_n \times \phi_n \times r^n \times s^{N-n}}{\sum_{j=0}^N M_j \times \phi_j \times r^j s^{N-j}} = \frac{\frac{N!}{n!(N-n)!} \times r^n \times s^{N-n}}{\sum_{j=0}^N \frac{N!}{j!(N-j)!} \times r^j \times s^{N-j}} = \frac{N!}{n!(N-n)!} \times \frac{r^n \times s^{N-n}}{(r+s)^N} \quad (5) \\ &= \frac{N!}{n!(N-n)!} \times X_R^n \times (1-X_R)^{N-n} \end{aligned}$$

The experimental NMR signal measures linear combinations of X_n . For the specific case of $N = 6$,

$$\text{Mole fraction of } [R_0S_6] + [R_6S_0] = X_0 + X_6$$

$$\text{Mole fraction of } [R_1S_5] + [R_5S_1] = X_1 + X_5$$

$$\text{Mole fraction of } [R_2S_4] + [R_4S_2] = X_2 + X_4$$

$$\text{Mole fraction of } [R_3S_3] = X_3$$

Using eq 5 these are equal to,

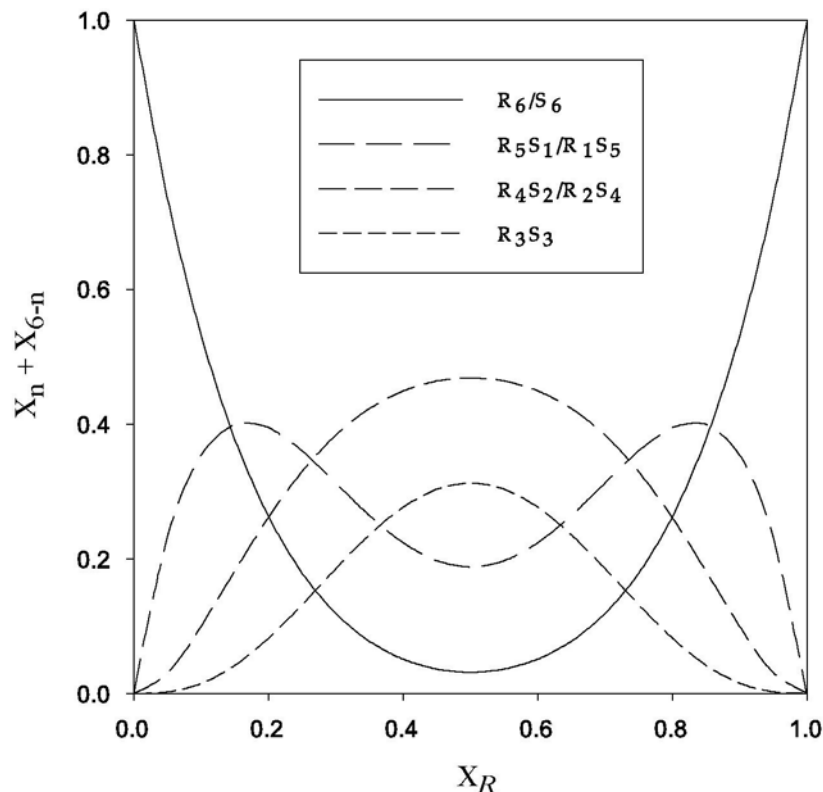
$$\text{Mole fraction of } [R_0S_6] + [R_6S_0] = X_R^6 + (1 - X_R)^6$$

$$\text{Mole fraction of } [R_1S_5] + [R_5S_1] = 6X_R^5(1 - X_R) + 6X_R(1 - X_R)^5$$

$$\text{Mole fraction of } [R_2S_4] + [R_4S_2] = 15X_R^4(1 - X_R)^2 + 15X_R^2(1 - X_R)^4$$

$$\text{Mole fraction of } [R_3S_3] = 20X_R^3(1 - X_R)^3$$

The above formulae are used to plot all four populations as a function of X_R . Because there are no free parameters, the experimental data either matches this plot, or the assumption that ϕ_n does not depend on n is wrong.



VI. The Parametric Method: In general, each permutation can differ in stability, so ϕ_n depends on n . In this case, there is not a simple analytic expression for X_n as a function of X_R and ϕ_n . However, eqs 2 and 3 permit one to evaluate X_R and X_n as functions of r/s . For example, when $N = 6$, the total mole fraction of R is

$$X_R = \frac{\sum_{n=0}^N n M_n \phi_n r^n s^{N-n}}{\sum_{n=0}^N N M_n \phi_n r^n s^{N-n}} = \frac{\phi_1 r^1 s^5 + 5\phi_2 r^2 s^4 + 10\phi_3 r^3 s^3 + 10\phi_4 r^4 s^2 + 5\phi_5 r^5 s^1 + \phi_6 r^6}{\phi_0 s^6 + 6\phi_1 r^1 s^5 + 15\phi_2 r^2 s^4 + 20\phi_3 r^3 s^3 + 15\phi_4 r^4 s^2 + 6\phi_5 r^5 s^1 + \phi_6 r^6} \quad (6)$$

and the experimentally measured mole fractions, X_n , are

$$X_0 + X_6 = \frac{\phi_0 s^6 + \phi_6 r^6}{\phi_0 s^6 + 6\phi_1 r^1 s^5 + 15\phi_2 r^2 s^4 + 20\phi_3 r^3 s^3 + 15\phi_4 r^4 s^2 + 6\phi_5 r^5 s^1 + \phi_6 r^6} \quad (7)$$

$$X_1 + X_5 = \frac{6(\phi_1 r^1 s^5 + \phi_5 r^5 s^1)}{\phi_0 s^6 + 6\phi_1 r^1 s^5 + 15\phi_2 r^2 s^4 + 20\phi_3 r^3 s^3 + 15\phi_4 r^4 s^2 + 6\phi_5 r^5 s^1 + \phi_6 r^6} \quad (8)$$

$$X_2 + X_4 = \frac{15(\phi_2 r^2 s^4 + \phi_4 r^4 s^2)}{\phi_0 s^6 + 6\phi_1 r^1 s^5 + 15\phi_2 r^2 s^4 + 20\phi_3 r^3 s^3 + 15\phi_4 r^4 s^2 + 6\phi_5 r^5 s^1 + \phi_6 r^6} \quad (9)$$

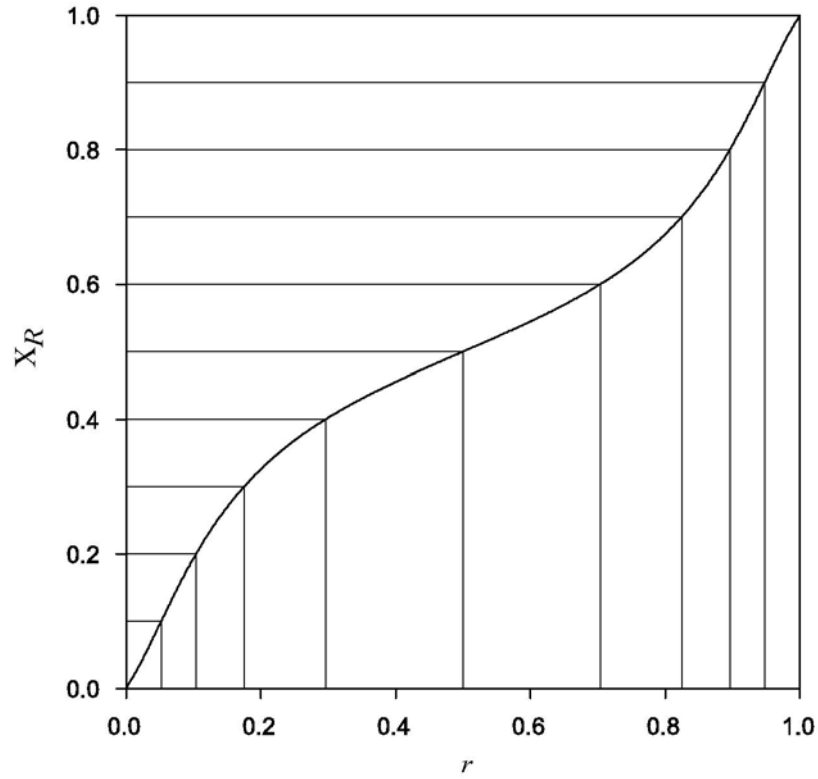
$$X_3 = \frac{20\phi_3 r^3 s^3}{\phi_0 s^6 + 6\phi_1 r^1 s^5 + 15\phi_2 r^2 s^4 + 20\phi_3 r^3 s^3 + 15\phi_4 r^4 s^2 + 6\phi_5 r^5 s^1 + \phi_6 r^6} \quad (10)$$

For a given value of X_R and ϕ_n , one may determine the required value of r/s via numeric inversion of eq 6 or by graphing X_R versus r . Using the obtained value r/s and eqs 7-10, one can then compute the populations. A graphical depiction of the parametric approach is described below for the case where $\phi_0 = \phi_6 = 1$, $\phi_1 = \phi_5 = 1.5$, $\phi_2 = \phi_4 = 5$, $\phi_3 = 10$.

Since the above equations only depend on the ratio, r/s , for convenience we may define

$$s = 1 - r \quad \leftrightarrow \quad \frac{r}{s} = \frac{r}{1-r}$$

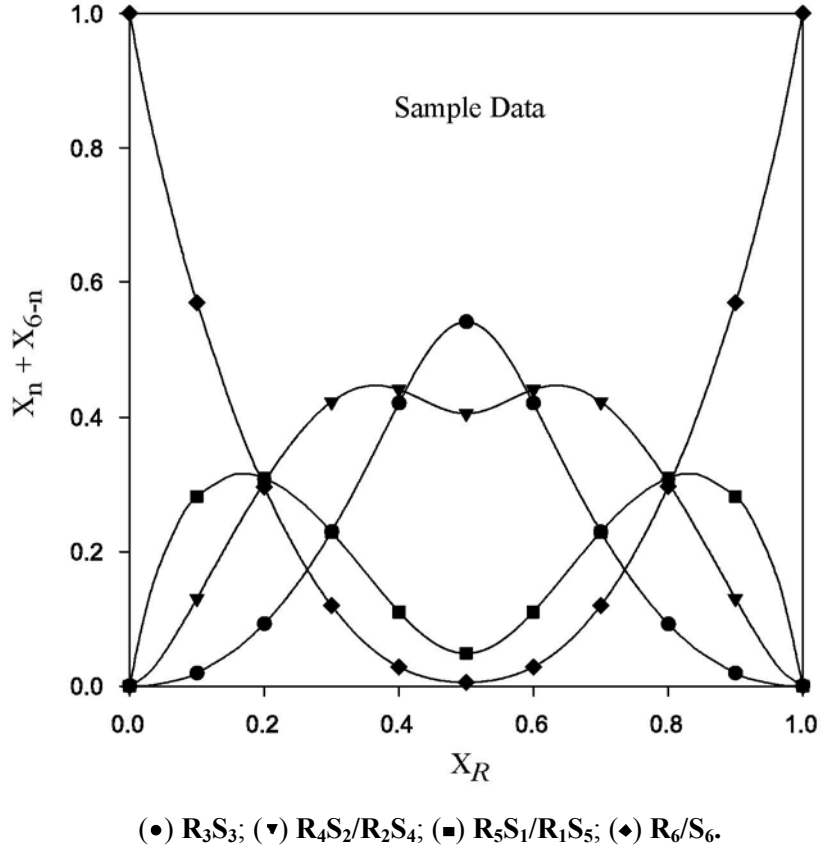
Using eq 6, we obtain the following plot for the example where $\varphi_0 = \varphi_6 = 1$, $\varphi_1 = \varphi_5 = 1.5$, $\varphi_2 = \varphi_4 = 5$, $\varphi_3 = 10$.



The drop lines depicted for each X_R allow one to determine the corresponding value of r . For this example we obtain the following values of r at each X_R .

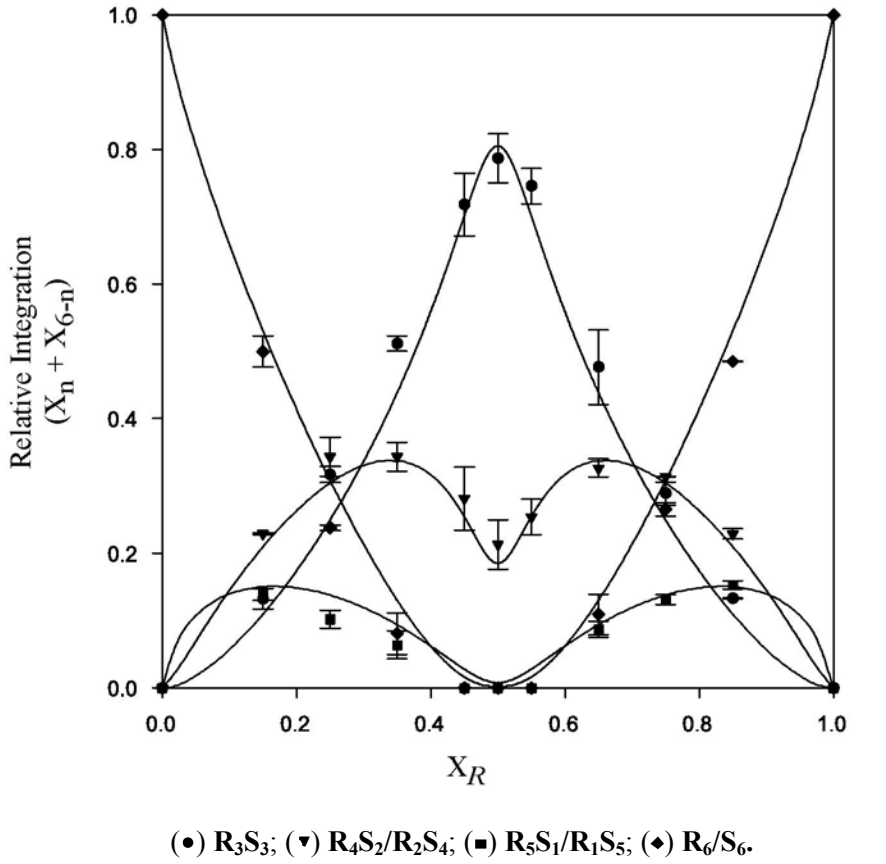
X_R	r	r/s
0	0	0
0.1	0.0522	0.0551
0.2	0.104	0.116
0.3	0.175	0.213
0.4	0.296	0.421
0.5	0.50	1.0
0.6	0.704	2.377
0.7	0.825	4.706
0.8	0.896	8.643
0.9	0.948	18.14
1.0	1.0	infinity

Using these values of r/s , we compute $X_0 + X_6$, $X_1 + X_5$, $X_2 + X_4$, and X_3 using eqs 7-10. The results are plotted below.



Comparing the above plot with the plot obtained in the statistical case (Section V), there are several notable changes. For instance, at $X_R = 0.5$, R_3S_3 exhibits a maximum and is now the dominant species. This result matches our expectations because φ_3 was set to be larger than all other φ_n 's ($\varphi_0 = \varphi_6 = 1$, $\varphi_1 = \varphi_5 = 1.5$, $\varphi_2 = \varphi_4 = 5$, $\varphi_3 = 10$).

VII. Fitting the Experimental Data with the Parametric Method: To compare the theory directly to experiment, one can refine an initial guess of ϕ_n until the predicted populations for the experimental values of X_R best fit the experimental populations. An adaptive step algorithm iteratively adjusts ϕ_n to minimize the root mean square error in the predicted populations. $N/2$ of the ϕ_n variables are independent, and for $N = 6$, ϕ_1 , ϕ_2 , and ϕ_3 are a convenient choice. A software package that supports nonlinear least-squares fitting of parametric equations is required.



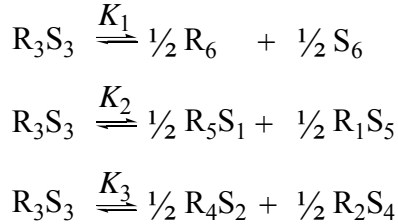
Best fit values of ϕ

ϕ_0	ϕ_1	ϕ_2	ϕ_3	ϕ_4	ϕ_5	ϕ_6
1.0	0.79	7.3	47.7	7.3	0.79	1.0

Percent Errors in ϕ_n

n	0	1	2	3
ϕ_n/ϕ_0	0	3.7	6.5	9.4
ϕ_n/ϕ_1	3.7	0	3.7	6.5
ϕ_n/ϕ_2	6.5	3.7	0	2.8
ϕ_n/ϕ_3	9.4	6.5	2.8	0

VIII. Equilibrium Constants: The “free energy coefficients” ϕ_n , of R_nS_{N-n} , are related to the equilibrium constants as follows



We now express K_1 , K_2 and K_3 in terms of ϕ_n using eq 1.

$$K_1 = \frac{[R_6]^{1/2} \times [S_6]^{1/2}}{[R_3S_3]}$$

Substituting the three concentrations into eq 1

$$[S_6] = C \times M_0 \times \phi_0 \times s^6 \quad [R_6] = C \times M_6 \times \phi_6 \times r^6 \quad [R_3S_3] = C \times M_3 \times \phi_3 \times r^3 \times s^3$$

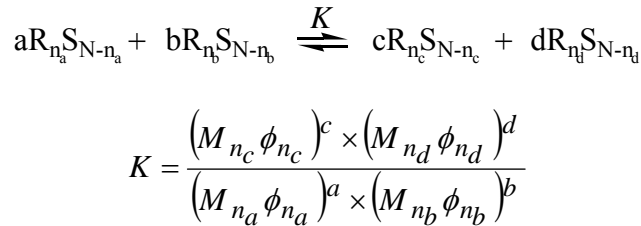
which then give,

$$K_1 = \frac{(CM_0\phi_0s^6)^{1/2} \times (CM_6\phi_6r^6)^{1/2}}{(CM_3\phi_3r^3s^3)} = \frac{\phi_0}{20\phi_3}$$

For the above reactions,

$$K_1 = \frac{\phi_0}{20\phi_3} \quad K_2 = \frac{3\phi_1}{10\phi_3} \quad K_3 = \frac{3\phi_2}{4\phi_3}$$

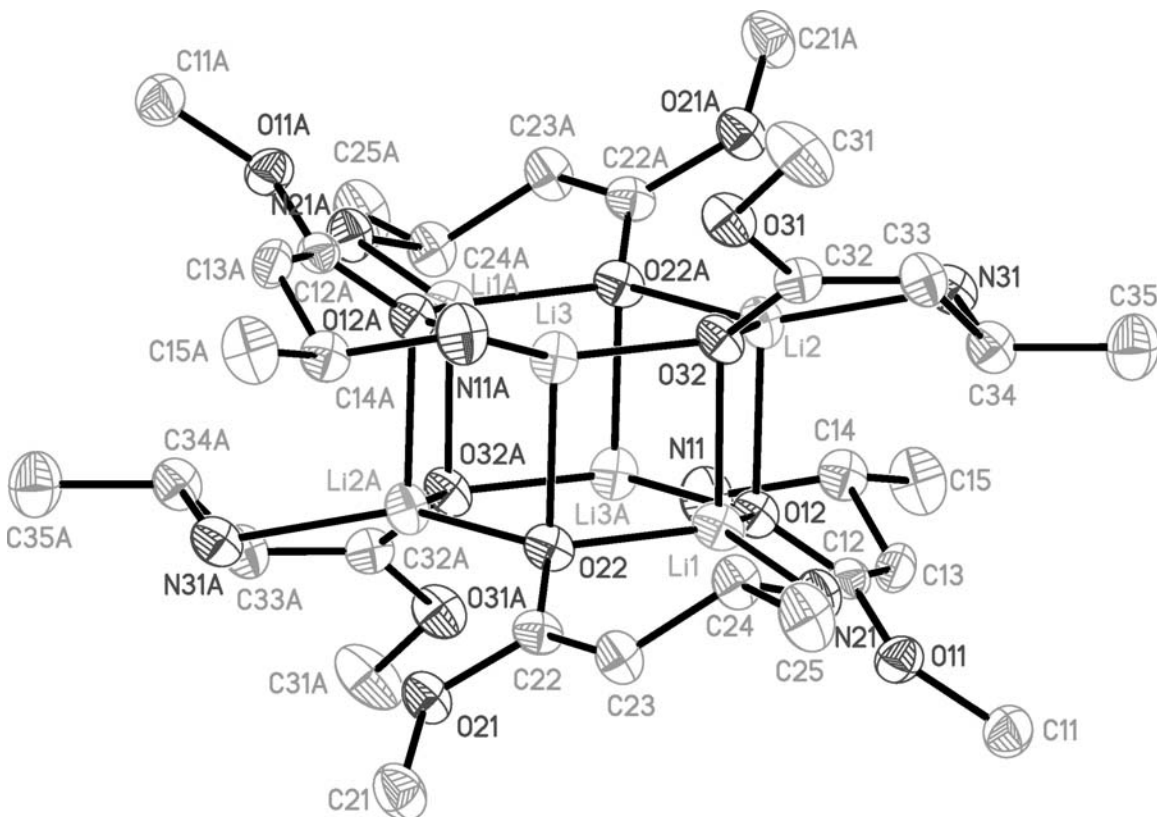
For the general case,



K_{statistical}		ΔG_{statistical}^a	(kcal/mol)
<i>K</i> ₁	0.05	Δ <i>G</i> ₁	1.33
<i>K</i> ₂	0.30	Δ <i>G</i> ₂	0.53
<i>K</i> ₃	0.75	Δ <i>G</i> ₃	0.13
K_{experimental}		ΔG_{non-statistical}^b	(kcal/mol)
<i>K</i> ₁	$1.0 \pm 0.1 \times 10^{-3}$	Δ <i>G</i> ₁	1.73 ± 0.04
<i>K</i> ₂	$5.0 \pm 0.3 \times 10^{-3}$	Δ <i>G</i> ₂	1.82 ± 0.03
<i>K</i> ₃	$115 \pm 3 \times 10^{-3}$	Δ <i>G</i> ₃	0.83 ± 0.01

a. $\Delta G_{\text{statistical}} = -RT\ln K_{\text{statistical}}$ where $R = 0.001987 \text{ kcal/mol}\text{K}$ and $T = 223.15 \text{ K}$. b. $\Delta G_{\text{non-statistical}} = -RT\ln K_n/K_{\text{statistical}}$

Crystal Structure



I. Crystals of *rac*-**1** were obtained from a 0.20 M enolate solution in 9.0 M THF/toluene held at -20 °C over 24 h. Single crystals suitable for X-ray diffraction were coated with polyisobutylene oil in a glovebox and were quickly transferred to the goniometer head of a Siemens SMART ($\lambda = 0.71073 \text{ \AA}$ T=173 K). The crystal belongs to the space group P1(bar). 1818 frames were collected using 0.3 deg. omega scans ($2\theta_{\max} = 46.52^\circ$). The data were processed with Bruker SAINT and SADABS programs to yield a total of 6120 unique reflections ($R(\text{int})=0.0575$). The structure was solved using direct method (SHELXS) completed by subsequent Fourier synthesis and refined by full-matrix least-squares procedures (SHELXL). At final convergence, $R(1) = 0.0665$ for 3433 $F_o > 4\text{sig}(F_o)$ and GOF = 0.949 for 772 parameters.

II. Crystal data and structure refinement.

Identification code	am1	
Empirical formula	C15 H30 Li3 N3 O6	
Formula weight	369.24	
Temperature	173(2) K	
Wavelength	0.71073 Å	
Crystal system	Triclinic	
Space group	P-1	
Unit cell dimensions	a = 13.423(11) Å b = 13.495(12) Å c = 13.817(12) Å	α= 91.83(3)°. β= 104.60(2)°. γ = 111.29(3)°.
Volume	2235(3) Å ³	
Z	4	
Density (calculated)	1.097 Mg/m ³	
Absorption coefficient	0.081 mm ⁻¹	
F(000)	792	
Crystal size	0.40 x 0.20 x 0.10 mm ³	
Theta range for data collection	1.63 to 23.26°.	
Index ranges	-13<=h<=14, -14<=k<=14, -14<=l<=15	
Reflections collected	9964	
Independent reflections	6120 [R(int) = 0.0575]	
Completeness to theta = 23.26°	95.6 %	
Absorption correction	SADABS	
Max. and min. transmission	0.9920 and 0.9684	
Refinement method	Full-matrix least-squares on F ²	
Data / restraints / parameters	6120 / 0 / 772	
Goodness-of-fit on F ²	0.949	
Final R indices [I>2sigma(I)]	R1 = 0.0665, wR2 = 0.1502	
R indices (all data)	R1 = 0.1275, wR2 = 0.1793	
Largest diff. peak and hole	0.249 and -0.284 e.Å ⁻³	

III. Table of Bond lengths [Å] and Angles [°].

O(11)-C(12)	1.369(5)	Li(2)-Li(3)#1	2.677(9)
O(11)-C(11)	1.414(6)	Li(2)-Li(1)#1	3.307(10)
O(12)-C(12)	1.304(5)	Li(2)-Li(3)	3.502(9)
O(12)-Li(3)#1	1.933(8)	Li(3)-O(12)#1	1.933(8)
O(12)-Li(1)	1.985(7)	Li(3)-N(11)#1	2.086(8)
O(12)-Li(2)	2.046(8)	Li(3)-Li(2)#1	2.677(9)
O(21)-C(22)	1.366(5)	Li(3)-Li(1)#1	3.333(9)
O(21)-C(21)	1.410(6)	O(11')-C(12')	1.379(5)
O(22)-C(22)	1.294(5)	O(11')-C(11')	1.411(5)
O(22)-Li(2)#1	1.915(7)	O(12')-C(12')	1.306(4)
O(22)-Li(1)	1.946(7)	O(12')-Li(1')	1.952(7)
O(22)-Li(3)	2.031(8)	O(12')-Li(3')#2	1.997(8)
O(31)-C(32)	1.406(5)	O(12')-Li(2')	2.008(7)
O(31)-C(31)	1.429(5)	O(21')-C(22')	1.428(5)
O(31)-Li(3)	2.557(7)	O(21')-C(21')	1.430(6)
O(32)-C(32)	1.309(5)	O(22')-C(22')	1.305(5)
O(32)-Li(3)	1.938(7)	O(22')-Li(2')#2	1.957(8)
O(32)-Li(2)	1.961(7)	O(22')-Li(1')	1.977(7)
O(32)-Li(1)	1.995(7)	O(22')-Li(3')	1.994(7)
N(11)-C(14)	1.474(6)	O(31')-C(32')	1.385(4)
N(11)-Li(3)#1	2.086(8)	O(31')-C(31')	1.421(6)
N(21)-C(24)	1.493(6)	O(31')-Li(3')	2.660(7)
N(21)-Li(1)	2.054(8)	O(32')-C(32')	1.298(4)
N(31)-C(34)	1.506(6)	O(32')-Li(2')	1.927(7)
N(31)-Li(2)	2.038(8)	O(32')-Li(3')	1.966(7)
C(12)-C(13)	1.371(6)	O(32')-Li(1')	2.029(7)
C(13)-C(14)	1.501(6)	N(11')-C(14')	1.513(5)
C(14)-C(15)	1.539(7)	N(11')-Li(3')#2	2.045(7)
C(22)-C(23)	1.341(6)	N(21')-C(24')	1.488(5)
C(22)-Li(1)	2.766(8)	N(21')-Li(1')	2.079(8)
C(23)-C(24)	1.477(6)	N(31')-C(34')	1.480(6)
C(24)-C(25)	1.532(6)	N(31')-Li(2')	2.060(8)
C(32)-C(33)	1.320(6)	C(12')-C(13')	1.343(6)
C(32)-Li(3)	2.700(8)	C(13')-C(14')	1.483(6)
C(32)-Li(2)	2.774(8)	C(14')-C(15')	1.524(6)
C(33)-C(34)	1.531(6)	C(22')-C(23')	1.328(6)
C(34)-C(35)	1.500(7)	C(23')-C(24')	1.526(6)
Li(1)-Li(2)	2.712(10)	C(24')-C(25')	1.501(7)
Li(1)-Li(3)	2.721(10)	C(32')-C(33')	1.355(6)
Li(1)-Li(2)#1	3.307(10)	C(32')-Li(2')	2.783(8)
Li(1)-Li(3)#1	3.333(9)	C(33')-C(34')	1.481(6)
Li(2)-O(22)#1	1.915(7)	C(34')-C(35')	1.559(7)

Li(1')-Li(3')	2.681(9)	C(31)-O(31)-Li(3)	158.0(3)
Li(1')-Li(2')	2.725(10)	C(32)-O(32)-Li(3)	111.0(3)
Li(1')-Li(3')#2	3.391(11)	C(32)-O(32)-Li(2)	114.6(3)
Li(1')-Li(2')#2	3.461(10)	Li(3)-O(32)-Li(2)	127.9(3)
Li(2')-O(22')#2	1.957(8)	C(32)-O(32)-Li(1)	124.8(3)
Li(2')-Li(3')#2	2.664(9)	Li(3)-O(32)-Li(1)	87.5(3)
Li(2')-Li(3')	3.369(9)	Li(2)-O(32)-Li(1)	86.6(3)
Li(2')-Li(1')#2	3.461(10)	C(14)-N(11)-Li(3)#1	108.4(3)
Li(3')-O(12')#2	1.997(8)	C(24)-N(21)-Li(1)	107.8(4)
Li(3')-N(11')#2	2.045(7)	C(34)-N(31)-Li(2)	105.0(3)
Li(3')-Li(2')#2	2.664(9)	O(12)-C(12)-O(11)	110.4(3)
Li(3')-Li(1')#2	3.391(11)	O(12)-C(12)-C(13)	126.1(4)
C(1S)-C(2S)	0.90(5)	O(11)-C(12)-C(13)	123.5(4)
C(1S)-C(5S)#3	1.13(6)	C(12)-C(13)-C(14)	122.7(4)
C(1S)-C(4S)#3	1.61(6)	N(11)-C(14)-C(13)	110.3(4)
C(1S)-C(3S)	1.82(4)	N(11)-C(14)-C(15)	112.1(4)
C(2S)-C(3S)	1.111(18)	C(13)-C(14)-C(15)	110.7(4)
C(2S)-C(5S)#3	1.43(3)	O(22)-C(22)-C(23)	127.6(4)
C(2S)-C(5S)	1.62(3)	O(22)-C(22)-O(21)	110.1(3)
C(3S)-C(5S)	1.29(2)	C(23)-C(22)-O(21)	122.3(4)
C(3S)-C(4S)	1.90(3)	O(22)-C(22)-Li(1)	39.3(2)
C(4S)-C(5S)	1.17(2)	C(23)-C(22)-Li(1)	95.1(3)
C(4S)-C(1S)#3	1.61(6)	O(21)-C(22)-Li(1)	136.2(3)
C(5S)-C(1S)#3	1.13(6)	C(22)-C(23)-C(24)	120.4(4)
C(5S)-C(2S)#3	1.43(3)	C(23)-C(24)-N(21)	110.2(4)
C(5S)-C(5S)#3	1.98(5)	C(23)-C(24)-C(25)	111.0(4)
		N(21)-C(24)-C(25)	112.6(4)
C(12)-O(11)-C(11)	119.0(4)	O(32)-C(32)-C(33)	125.1(4)
C(12)-O(12)-Li(3)#1	117.9(3)	O(32)-C(32)-O(31)	109.5(3)
C(12)-O(12)-Li(1)	119.7(3)	C(33)-C(32)-O(31)	125.4(4)
Li(3)#1-O(12)-Li(1)	116.6(3)	O(32)-C(32)-Li(3)	42.1(2)
C(12)-O(12)-Li(2)	123.8(3)	C(33)-C(32)-Li(3)	162.0(4)
Li(3)#1-O(12)-Li(2)	84.5(3)	O(31)-C(32)-Li(3)	69.0(2)
Li(1)-O(12)-Li(2)	84.6(3)	O(32)-C(32)-Li(2)	40.0(2)
C(22)-O(21)-C(21)	116.7(4)	C(33)-C(32)-Li(2)	93.1(3)
C(22)-O(22)-Li(2)#1	119.8(3)	O(31)-C(32)-Li(2)	134.9(3)
C(22)-O(22)-Li(1)	115.8(3)	Li(3)-C(32)-Li(2)	79.6(2)
Li(2)#1-O(22)-Li(1)	117.9(3)	C(32)-C(33)-C(34)	122.1(4)
C(22)-O(22)-Li(3)	123.3(3)	C(35)-C(34)-N(31)	111.8(4)
Li(2)#1-O(22)-Li(3)	85.4(3)	C(35)-C(34)-C(33)	112.5(4)
Li(1)-O(22)-Li(3)	86.3(3)	N(31)-C(34)-C(33)	109.8(4)
C(32)-O(31)-C(31)	117.5(4)	O(22)-Li(1)-O(12)	124.2(3)
C(32)-O(31)-Li(3)	80.2(3)	O(22)-Li(1)-O(32)	93.5(3)

O(12)-Li(1)-O(32)	94.8(3)	O(12)-Li(2)-Li(3)#1	46.0(2)
O(22)-Li(1)-N(21)	97.4(3)	O(22)#1-Li(2)-Li(1)	112.6(3)
O(12)-Li(1)-N(21)	133.5(4)	O(32)-Li(2)-Li(1)	47.2(2)
O(32)-Li(1)-N(21)	103.0(3)	N(31)-Li(2)-Li(1)	105.2(3)
O(22)-Li(1)-Li(2)	117.8(4)	O(12)-Li(2)-Li(1)	46.8(2)
O(12)-Li(1)-Li(2)	48.7(2)	Li(3)#1-Li(2)-Li(1)	76.4(3)
O(32)-Li(1)-Li(2)	46.2(2)	O(22)#1-Li(2)-C(32)	130.5(3)
N(21)-Li(1)-Li(2)	131.1(3)	O(32)-Li(2)-C(32)	25.42(14)
O(22)-Li(1)-Li(3)	48.1(2)	N(31)-Li(2)-C(32)	76.9(2)
O(12)-Li(1)-Li(3)	119.0(3)	O(12)-Li(2)-C(32)	109.2(3)
O(32)-Li(1)-Li(3)	45.4(2)	Li(3)#1-Li(2)-C(32)	136.5(3)
N(21)-Li(1)-Li(3)	103.6(3)	Li(1)-Li(2)-C(32)	64.9(2)
Li(2)-Li(1)-Li(3)	80.3(3)	O(22)#1-Li(2)-Li(1)#1	31.32(18)
O(22)-Li(1)-C(22)	24.90(14)	O(32)-Li(2)-Li(1)#1	84.2(3)
O(12)-Li(1)-C(22)	138.8(3)	N(31)-Li(2)-Li(1)#1	166.6(4)
O(32)-Li(1)-C(22)	108.1(3)	O(12)-Li(2)-Li(1)#1	90.5(3)
N(21)-Li(1)-C(22)	74.7(2)	Li(3)#1-Li(2)-Li(1)#1	52.8(2)
Li(2)-Li(1)-C(22)	142.0(3)	Li(1)-Li(2)-Li(1)#1	87.1(3)
Li(3)-Li(1)-C(22)	64.9(2)	C(32)-Li(2)-Li(1)#1	104.1(2)
O(22)-Li(1)-Li(2)#1	30.78(18)	O(22)#1-Li(2)-Li(3)	89.5(3)
O(12)-Li(1)-Li(2)#1	94.5(3)	O(32)-Li(2)-Li(3)	25.89(17)
O(32)-Li(1)-Li(2)#1	88.3(3)	N(31)-Li(2)-Li(3)	125.6(3)
N(21)-Li(1)-Li(2)#1	128.1(3)	O(12)-Li(2)-Li(3)	90.5(3)
Li(2)-Li(1)-Li(2)#1	92.9(3)	Li(3)#1-Li(2)-Li(3)	90.7(3)
Li(3)-Li(1)-Li(2)#1	51.6(2)	Li(1)-Li(2)-Li(3)	50.0(2)
C(22)-Li(1)-Li(2)#1	53.88(19)	C(32)-Li(2)-Li(3)	49.30(18)
O(22)-Li(1)-Li(3)#1	94.1(3)	Li(1)#1-Li(2)-Li(3)	58.54(19)
O(12)-Li(1)-Li(3)#1	31.24(18)	O(12)#1-Li(3)-O(32)	115.0(3)
O(32)-Li(1)-Li(3)#1	88.9(3)	O(12)#1-Li(3)-O(22)	95.0(3)
N(21)-Li(1)-Li(3)#1	162.8(4)	O(32)-Li(3)-O(22)	92.6(3)
Li(2)-Li(1)-Li(3)#1	51.3(2)	O(12)#1-Li(3)-N(11)#1	97.9(3)
Li(3)-Li(1)-Li(3)#1	93.6(3)	O(32)-Li(3)-N(11)#1	140.8(4)
C(22)-Li(1)-Li(3)#1	113.7(3)	O(22)-Li(3)-N(11)#1	105.6(3)
Li(2)#1-Li(1)-Li(3)#1	63.7(2)	O(12)#1-Li(3)-O(31)	131.6(4)
O(22)#1-Li(2)-O(32)	114.7(4)	O(32)-Li(3)-O(31)	57.2(2)
O(22)#1-Li(2)-N(31)	140.2(4)	O(22)-Li(3)-O(31)	130.8(3)
O(32)-Li(2)-N(31)	99.9(3)	N(11)#1-Li(3)-O(31)	85.4(3)
O(22)#1-Li(2)-O(12)	95.1(3)	O(12)#1-Li(3)-Li(2)#1	49.5(2)
O(32)-Li(2)-O(12)	94.0(3)	O(32)-Li(3)-Li(2)#1	110.3(3)
N(31)-Li(2)-O(12)	101.9(4)	O(22)-Li(3)-Li(2)#1	45.5(2)
O(22)#1-Li(2)-Li(3)#1	49.1(2)	N(11)#1-Li(3)-Li(2)#1	107.1(3)
O(32)-Li(2)-Li(3)#1	111.4(3)	O(31)-Li(3)-Li(2)#1	167.4(3)
N(31)-Li(2)-Li(3)#1	134.8(4)	O(12)#1-Li(3)-C(32)	131.7(3)

O(32)-Li(3)-C(32)	26.91(15)	C(32')-O(31')-C(31')	117.4(4)
O(22)-Li(3)-C(32)	108.8(3)	C(32')-O(31')-Li(3')	81.3(2)
N(11)#1-Li(3)-C(32)	114.2(3)	C(31')-O(31')-Li(3')	154.1(3)
O(31)-Li(3)-C(32)	30.88(13)	C(32')-O(32')-Li(2')	117.9(3)
Li(2)#1-Li(3)-C(32)	136.8(3)	C(32')-O(32')-Li(3')	117.2(3)
O(12)#1-Li(3)-Li(1)	112.9(3)	Li(2')-O(32')-Li(3')	119.9(3)
O(32)-Li(3)-Li(1)	47.1(2)	C(32')-O(32')-Li(1')	121.3(3)
O(22)-Li(3)-Li(1)	45.5(2)	Li(2')-O(32')-Li(1')	87.0(3)
N(11)#1-Li(3)-Li(1)	137.4(4)	Li(3')-O(32')-Li(1')	84.3(3)
O(31)-Li(3)-Li(1)	94.4(3)	C(14')-N(11')-Li(3')#2	108.0(3)
Li(2)#1-Li(3)-Li(1)	75.6(3)	C(24')-N(21')-Li(1')	105.9(3)
C(32)-Li(3)-Li(1)	65.8(2)	C(34')-N(31')-Li(2')	111.5(3)
O(12)#1-Li(3)-Li(1)#1	32.17(18)	O(12')-C(12')-C(13')	124.9(4)
O(32)-Li(3)-Li(1)#1	83.8(3)	O(12')-C(12')-O(11')	110.4(3)
O(22)-Li(3)-Li(1)#1	89.1(3)	C(13')-C(12')-O(11')	124.7(4)
N(11)#1-Li(3)-Li(1)#1	129.8(3)	C(12')-C(13')-C(14')	123.2(4)
O(31)-Li(3)-Li(1)#1	120.6(3)	C(13')-C(14')-N(11')	110.4(4)
Li(2)#1-Li(3)-Li(1)#1	52.3(2)	C(13')-C(14')-C(15')	112.3(4)
C(32)-Li(3)-Li(1)#1	105.1(2)	N(11')-C(14')-C(15')	112.5(4)
Li(1)-Li(3)-Li(1)#1	86.4(3)	O(22')-C(22')-C(23')	128.2(4)
O(12)#1-Li(3)-Li(2)	89.6(3)	O(22')-C(22')-O(21')	108.6(4)
O(32)-Li(3)-Li(2)	26.22(16)	C(23')-C(22')-O(21')	123.1(4)
O(22)-Li(3)-Li(2)	88.7(3)	C(22')-C(23')-C(24')	122.4(4)
N(11)#1-Li(3)-Li(2)	163.1(3)	N(21')-C(24')-C(25')	111.8(4)
O(31)-Li(3)-Li(2)	78.3(2)	N(21')-C(24')-C(23')	111.7(4)
Li(2)#1-Li(3)-Li(2)	89.3(3)	C(25')-C(24')-C(23')	111.6(4)
C(32)-Li(3)-Li(2)	51.15(17)	O(32')-C(32')-C(33')	128.7(4)
Li(1)-Li(3)-Li(2)	49.8(2)	O(32')-C(32')-O(31')	107.8(3)
Li(1)#1-Li(3)-Li(2)	57.8(2)	C(33')-C(32')-O(31')	123.5(4)
C(12')-O(11')-C(11')	117.1(4)	O(32')-C(32')-Li(2')	37.7(2)
C(12')-O(12')-Li(1')	119.7(3)	C(33')-C(32')-Li(2')	95.0(3)
C(12')-O(12')-Li(3')#2	114.9(3)	O(31')-C(32')-Li(2')	137.7(3)
Li(1')-O(12')-Li(3')#2	118.4(3)	C(32')-C(33')-C(34')	123.1(4)
C(12')-O(12')-Li(2')	125.7(3)	N(31')-C(34')-C(33')	110.5(4)
Li(1')-O(12')-Li(2')	86.9(3)	N(31')-C(34')-C(35')	113.0(4)
Li(3')#2-O(12')-Li(2')	83.4(3)	C(33')-C(34')-C(35')	111.6(4)
C(22')-O(21')-C(21')	116.4(4)	O(12')-Li(1')-O(22')	116.9(4)
C(22')-O(22')-Li(2')#2	118.0(3)	O(12')-Li(1')-O(32')	92.3(3)
C(22')-O(22')-Li(1')	115.3(3)	O(22')-Li(1')-O(32')	94.6(3)
Li(2')#2-O(22')-Li(1')	123.2(3)	O(12')-Li(1')-N(21')	138.8(4)
C(22')-O(22')-Li(3')	120.0(3)	O(22')-Li(1')-N(21')	99.5(3)
Li(2')#2-O(22')-Li(3')	84.8(3)	O(32')-Li(1')-N(21')	103.8(3)
Li(1')-O(22')-Li(3')	84.9(3)	O(12')-Li(1')-Li(3')	112.8(3)

O(22')-Li(1')-Li(3')	47.8(2)	O(22')#2-Li(2')-Li(3')	87.7(3)
O(32')-Li(1')-Li(3')	46.9(2)	O(12')-Li(2')-Li(3')	88.6(3)
N(21')-Li(1')-Li(3')	105.7(3)	N(31')-Li(2')-Li(3')	127.5(3)
O(12')-Li(1')-Li(2')	47.4(2)	Li(3')#2-Li(2')-Li(3')	87.7(3)
O(22')-Li(1')-Li(2')	112.9(3)	Li(1')-Li(2')-Li(3')	50.9(2)
O(32')-Li(1')-Li(2')	44.9(2)	C(32')-Li(2')-Li(3')	53.27(18)
N(21')-Li(1')-Li(2')	134.5(4)	O(32')-Li(2')-Li(1')#2	89.4(3)
Li(3')-Li(1')-Li(2')	77.1(3)	O(22')#2-Li(2')-Li(1')#2	28.53(17)
O(12')-Li(1')-Li(3')#2	31.19(18)	O(12')-Li(2')-Li(1')#2	90.7(3)
O(22')-Li(1')-Li(3')#2	86.8(3)	N(31')-Li(2')-Li(1')#2	160.6(4)
O(32')-Li(1')-Li(3')#2	86.8(3)	Li(3')#2-Li(2')-Li(1')#2	49.9(2)
N(21')-Li(1')-Li(3')#2	167.0(3)	Li(1')-Li(2')-Li(1')#2	90.7(3)
Li(3')-Li(1')-Li(3')#2	87.0(3)	C(32')-Li(2')-Li(1')#2	109.0(2)
Li(2')-Li(1')-Li(3')#2	50.2(2)	Li(3')-Li(2')-Li(1')#2	59.5(2)
O(12')-Li(1')-Li(2')#2	89.7(3)	O(32')-Li(3')-O(22')	96.1(3)
O(22')-Li(1')-Li(2')#2	28.23(18)	O(32')-Li(3')-O(12')#2	120.0(4)
O(32')-Li(1')-Li(2')#2	88.5(3)	O(22')-Li(3')-O(12')#2	95.5(3)
N(21')-Li(1')-Li(2')#2	127.7(3)	O(32')-Li(3')-N(11')#2	137.1(4)
Li(3')-Li(1')-Li(2')#2	49.4(2)	O(22')-Li(3')-N(11')#2	99.7(3)
Li(2')-Li(1')-Li(2')#2	89.3(3)	O(12')#2-Li(3')-N(11')#2	97.8(3)
Li(3')#2-Li(1')-Li(2')#2	58.89(19)	O(32')-Li(3')-O(31')	53.37(19)
O(32')-Li(2')-O(22')#2	116.8(3)	O(22')-Li(3')-O(31')	124.1(3)
O(32')-Li(2')-O(12')	93.7(3)	O(12')#2-Li(3')-O(31')	139.4(3)
O(22')#2-Li(2')-O(12')	96.3(3)	N(11')#2-Li(3')-O(31')	85.2(3)
O(32')-Li(2')-N(31')	97.4(3)	O(32')-Li(3')-Li(2')#2	117.0(3)
O(22')#2-Li(2')-N(31')	137.1(4)	O(22')-Li(3')-Li(2')#2	47.0(2)
O(12')-Li(2')-N(31')	106.9(4)	O(12')#2-Li(3')-Li(2')#2	48.5(2)
O(32')-Li(2')-Li(3')#2	113.2(3)	N(11')#2-Li(3')-Li(2')#2	102.7(3)
O(22')#2-Li(2')-Li(3')#2	48.2(2)	O(31')-Li(3')-Li(2')#2	168.7(3)
O(12')-Li(2')-Li(3')#2	48.1(2)	O(32')-Li(3')-Li(1')	48.9(2)
N(31')-Li(2')-Li(3')#2	139.6(4)	O(22')-Li(3')-Li(1')	47.3(2)
O(32')-Li(2')-Li(1')	48.1(2)	O(12')#2-Li(3')-Li(1')	117.9(3)
O(22')#2-Li(2')-Li(1')	114.5(3)	N(11')#2-Li(3')-Li(1')	130.5(4)
O(12')-Li(2')-Li(1')	45.7(2)	O(31')-Li(3')-Li(1')	88.0(3)
N(31')-Li(2')-Li(1')	107.4(3)	Li(2')#2-Li(3')-Li(1')	80.7(3)
Li(3')#2-Li(2')-Li(1')	78.0(3)	O(32')-Li(3')-Li(2')	29.75(18)
O(32')-Li(2')-C(32')	24.34(14)	O(22')-Li(3')-Li(2')	90.8(3)
O(22')#2-Li(2')-C(32')	132.5(3)	O(12')#2-Li(3')-Li(2')	91.6(3)
O(12')-Li(2')-C(32')	107.1(3)	N(11')#2-Li(3')-Li(2')	165.1(3)
N(31')-Li(2')-C(32')	74.2(3)	O(31')-Li(3')-Li(2')	80.1(2)
Li(3')#2-Li(2')-C(32')	137.1(3)	Li(2')#2-Li(3')-Li(2')	92.3(3)
Li(1')-Li(2')-C(32')	64.1(2)	Li(1')-Li(3')-Li(2')	52.0(2)
O(32')-Li(2')-Li(3')	30.40(18)	O(32')-Li(3')-Li(1')#2	90.8(3)

O(22')-Li(3')-Li(1')#2	90.8(3)	
O(12')#2-Li(3')-Li(1')#2	30.42(17)	Symmetry transformations used to generate equivalent atoms:
N(11')#2-Li(3')-Li(1')#2	128.2(3)	#1 -x+1,-y+2,-z #2 -x+1,-y+1,-z+1 #3 -x+2,-y+2,-z+1
O(31')-Li(3')-Li(1')#2	128.9(3)	
Li(2')#2-Li(3')-Li(1')#2	51.8(2)	
Li(1')-Li(3')-Li(1')#2	93.0(3)	
Li(2')-Li(3')-Li(1')#2	61.6(2)	
C(2S)-C(1S)-C(5S)#3	89(6)	
C(2S)-C(1S)-C(4S)#3	128(6)	
C(5S)#3-C(1S)-C(4S)#3	47(3)	
C(2S)-C(1S)-C(3S)	28(2)	
C(5S)#3-C(1S)-C(3S)	95(4)	
C(4S)#3-C(1S)-C(3S)	117(3)	
C(1S)-C(2S)-C(3S)	130(4)	
C(1S)-C(2S)-C(5S)#3	52(4)	
C(3S)-C(2S)-C(5S)#3	122.1(15)	
C(1S)-C(2S)-C(5S)	126(4)	
C(3S)-C(2S)-C(5S)	52.3(14)	
C(5S)#3-C(2S)-C(5S)	80.7(15)	
C(2S)-C(3S)-C(5S)	85(2)	
C(2S)-C(3S)-C(4S)	93(2)	
C(5S)-C(3S)-C(4S)	37.0(12)	
C(2S)-C(3S)-C(1S)	22(2)	
C(5S)-C(3S)-C(1S)	92.0(18)	
C(4S)-C(3S)-C(1S)	111(2)	
C(5S)-C(4S)-C(1S)#3	45(2)	
C(5S)-C(4S)-C(3S)	41.6(13)	
C(1S)#3-C(4S)-C(3S)	86(2)	
C(1S)#3-C(5S)-C(4S)	89(3)	
C(1S)#3-C(5S)-C(3S)	170(4)	
C(4S)-C(5S)-C(3S)	101(2)	
C(1S)#3-C(5S)-C(2S)#3	39(3)	
C(4S)-C(5S)-C(2S)#3	122(2)	
C(3S)-C(5S)-C(2S)#3	131(2)	
C(1S)#3-C(5S)-C(2S)	132(3)	
C(4S)-C(5S)-C(2S)	106.5(19)	
C(3S)-C(5S)-C(2S)	43.1(10)	
C(2S)#3-C(5S)-C(2S)	99.3(15)	
C(1S)#3-C(5S)-C(5S)#3	89(3)	
C(4S)-C(5S)-C(5S)#3	128(2)	
C(3S)-C(5S)-C(5S)#3	83.1(15)	
C(2S)#3-C(5S)-C(5S)#3	53.9(12)	
C(2S)-C(5S)-C(5S)#3	45.4(9)	